NASA CR-137581
Available to U.S. Government
Agencies and their Contractors

NOISE AND STATIC PERFORMANCE CHARACTERISTICS OF A STOL AIRCRAFT JET FLAP

D. L. Harkonen, J. F. McBride, J. V. O'Keefe

D6-42312
December 1974

Boeing Commercial Airplane Company
P.O. Box 3707
Seattle, Washington 98124

for
Ames Research Center
NATIONAL AERONAUTICS AND SPACE ADMINISTRATION
Washington, D.C. 20546

1. Report No.	2. Government Accession No.	3. Recipient's Catalog No.
NASA CR-137581		

4. Title and Subtitle	5. Report Date
Noise and Static Performance Characteristics of a STOL Aircraft Jet Flap	December 1974
	6. Performing Organization Code

7. Author(s)	8. Performing Organization Report No.
D. L. Harkonen, J. F. McBride, J. V. O'Keefe	D6-42312
	10. Work Unit No.

9. Performing Organization Name and Address	11. Contract or Grant No.
Boeing Commercial Airplane Company P.O. Box 3707 Seattle, Washington 98124	NAS 2-7641
	13. Type of Report and Period Covered
12. Sponsoring Agency Name and Address	Final Report
National Aeronautics Space Administration Washington, D.C. 20546	14. Sponsoring Agency Code

15. Supplementary Notes

16. Abstract

Static noise and performance tests were conducted on a 1/4-scale jet flap model with a multilobe nozzle of array area ratio of 2.7.

The model nozzle and flap tested were a two-dimensional section of a distributed blowing system similar to previously investigated augmentor wing systems without the upper shroud and intake door. Noise data were measured with the nozzle alone and also during attached flow conditions with the flap at two turning angles representing takeoff and approach conditions.

The noise data are scaled to a 200 000-lb TOGW four-engine airplane and are presented in terms of perceived noise level (PNL) and one-third octave band sound pressure level (SPL). Comparisons are made with the noise levels produced by an augmentor wing airplane fitted with a three-element acoustically lined augmentor flap. The static performance is presented in terms of thrust recovery and effective turning angle.

17. Key Words (Suggested by Author(s))	18. Distribution Statement
Jet flap Noise shielding Powered lift Interaction noise	Distribution is provided in the interest of information exchange. Responsibility for the contents resides in the author or organization that prepared it.

19. Security Classif. (of this report)	20. Security Classif. (of this page)	21. No. of Pages	22. Price*
Unclassified	Unclassified		

*For sale by the National Technical Information Service, Springfield, Virginia 22151

CONTENTS

SUMMARY

A 1/4-scale model jet flap and multi-element lobed nozzle were tested for static performance and far field noise characteristics. The model suppressor nozzle and flap represented a two-dimensional section of a distributed blowing system similar to an augmentor wing without the upper flap elements (shroud and intake door), see figure 1. The concept as it might apply to STOL aircraft is illustrated in figure 2.

The objective of the test was to measure and compare the far field noise produced by a small array-area-ratio (AAR) multilobe nozzle and flap with the noise levels previously measured with an acoustically lined augmentor flap model (ref. 1). The noise data were recorded during attached flow conditions with the flap at simulated takeoff and approach deflection angles. The nozzle and flap model were rotated with respect to the microphone array to simulate airplane flyover and sideline orientations.

Acoustic performance of the jet flap system is summarized in four figures. The measured spectra and perceived noise level (PNL) values in the figures are scaled and corrected to represent a four-engine 200 000-lb TOGW STOL airplane (150 passengers) operating on a standard day (77°F and 70% rh).

Figure 3 shows the effect of adding the jet flap system to the multilobe jet nozzle at the nominal takeoff jet velocity (nozzle pressure ratio 2.6). Significant high-frequency shielding is evident, but it is countered by some increase in low-frequency noise from apparent jet/flap flow interaction. The resulting peak sideline noise is some 4 to 5 PNdB quieter for the jet flap system than for the simple jet exhaust suppressed by multi-element nozzle array.

The effect of the experimental flap gap baffle is indicated in figure 4. The noise observed beneath the wing ($\beta = 0°$) was hardly affected by the baffle at the takeoff power and flap angle setting (NPR = 2.6, $\delta_F = 20°$) and only to the extent of 1 PNdB at the nominal approach condition (NPR = 1.6, $\delta_F = 65°$).

The best experimental augmentor wing model of the DNS Task V (see ref. 1) gave a scaled, corrected noise level at the 500-ft sideline of 96.8 PNdB, which was shown (page 2 of ref. 1) to give promise of a STOL airplane capable of producing less than 90 PNdB peak 500-ft sideline noise on takeoff. Figure 5 compares the scaled noise of the 70-lobe jet flap with the lowest noise lined augmentor wing configuration and with a hardwall version of this same 20-lobe corrugated nozzle system. The effect of augmentor flap and shroud lining is seen between 800 and 2500 Hz. Important spectral differences between the jet flap and augmentor flap systems are also evident; the

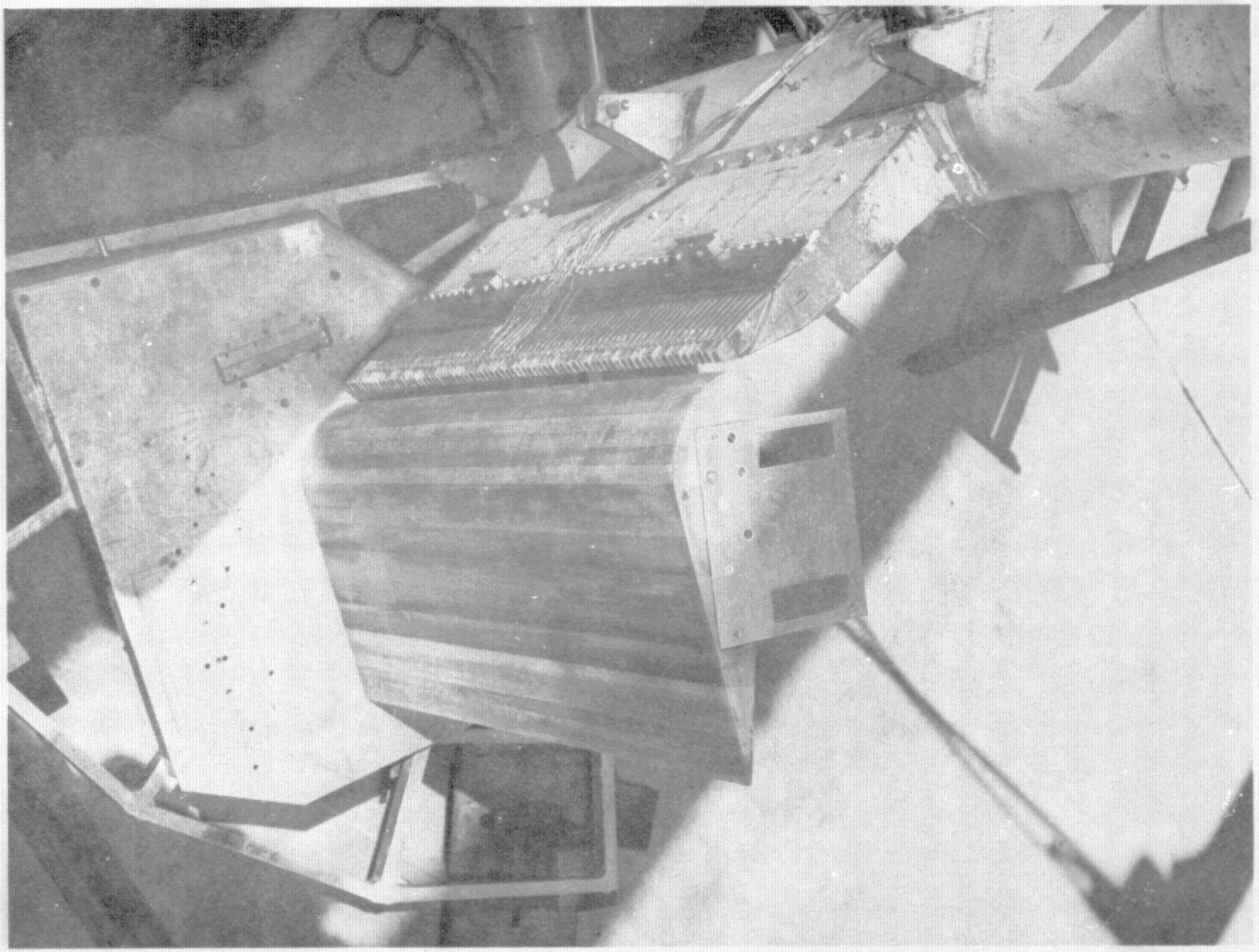

FIGURE 1.—JET FLAP MODEL WITH ONE END PLATE REMOVED, $\delta_F = 65°$

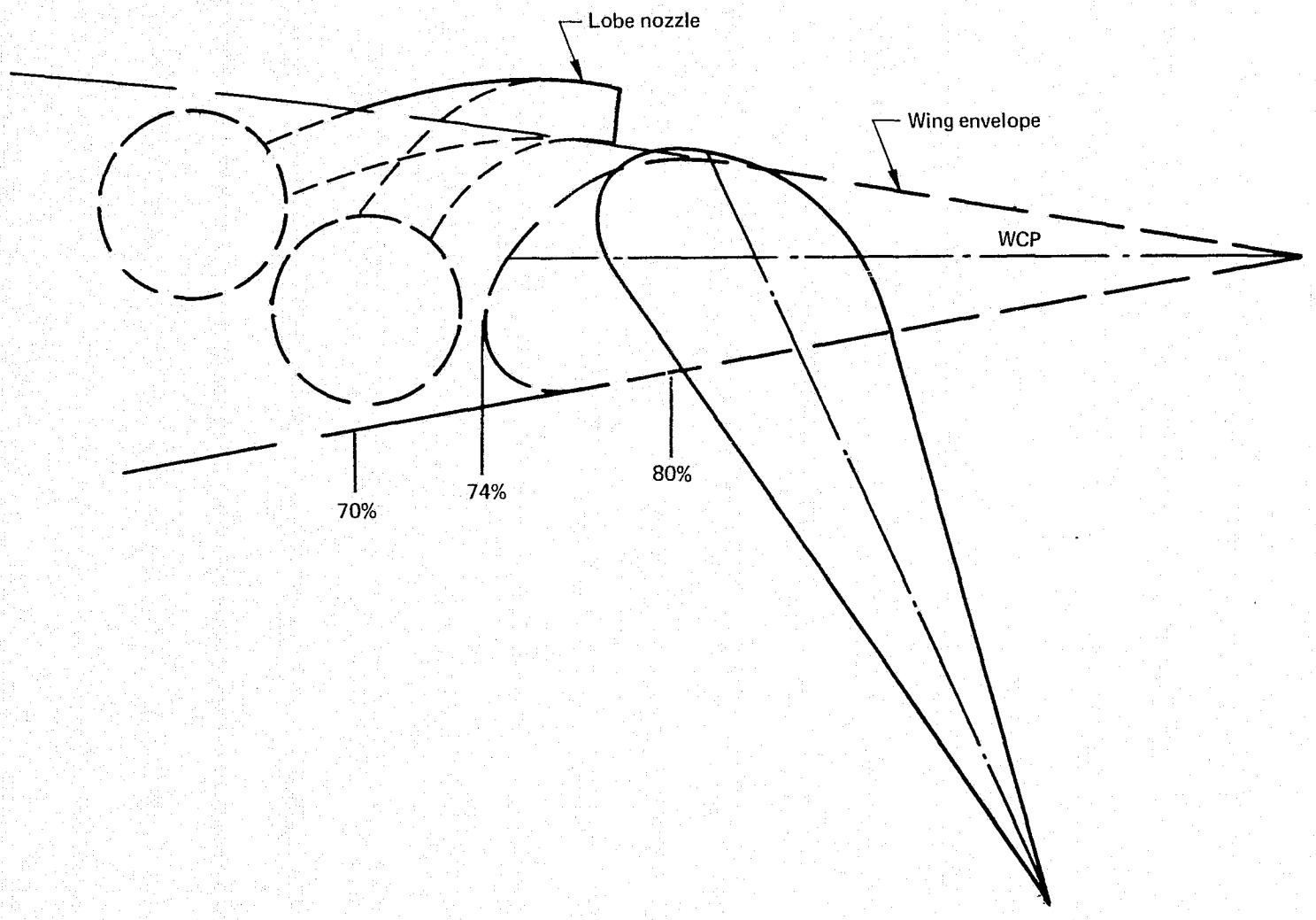

FIGURE 2.–JET FLAP–STOL AIRCRAFT INSTALLATION

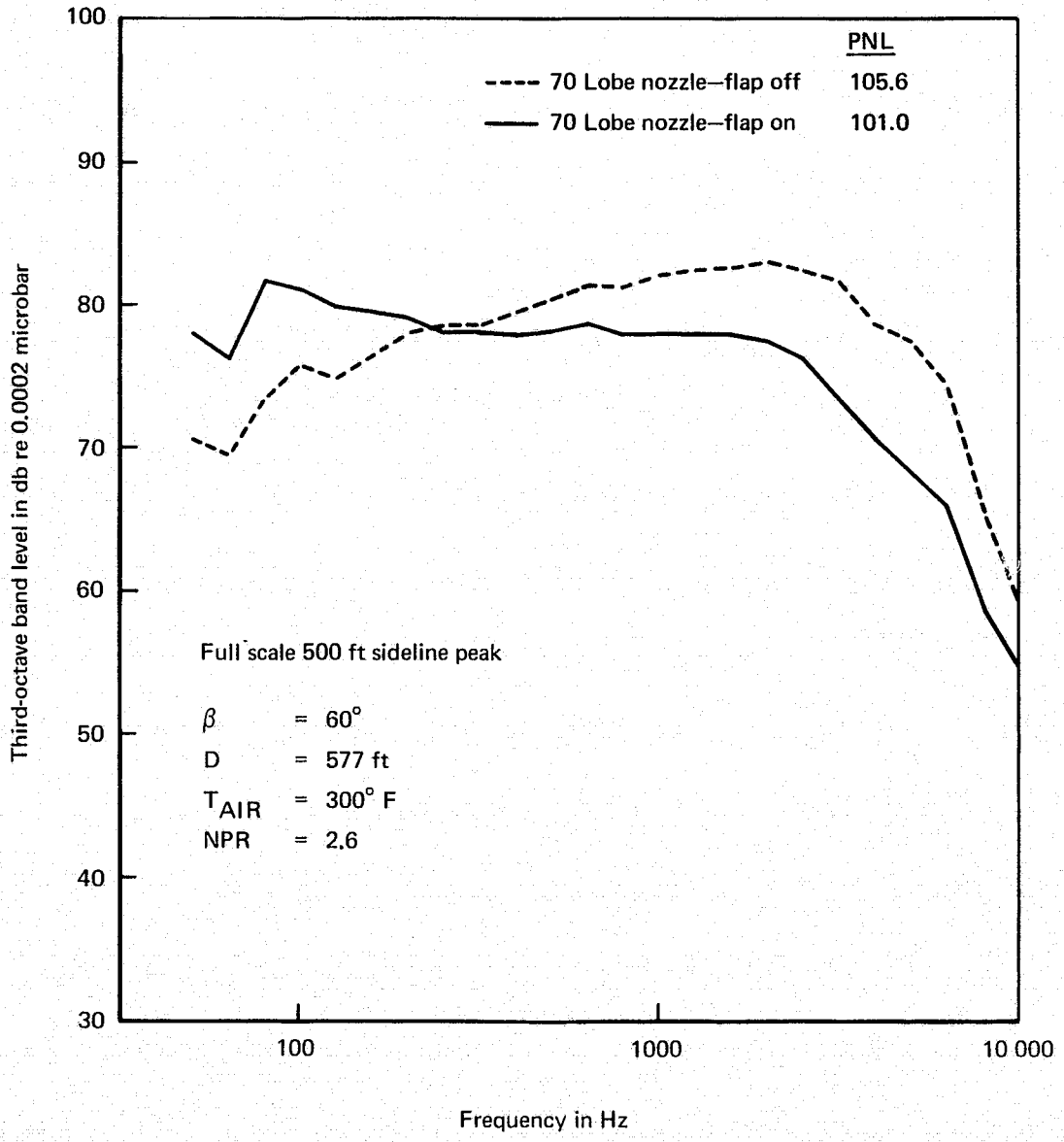

FIGURE 3.—EFFECT OF ADDING JET FLAP (TAKEOFF, $\delta_F = 20°$)

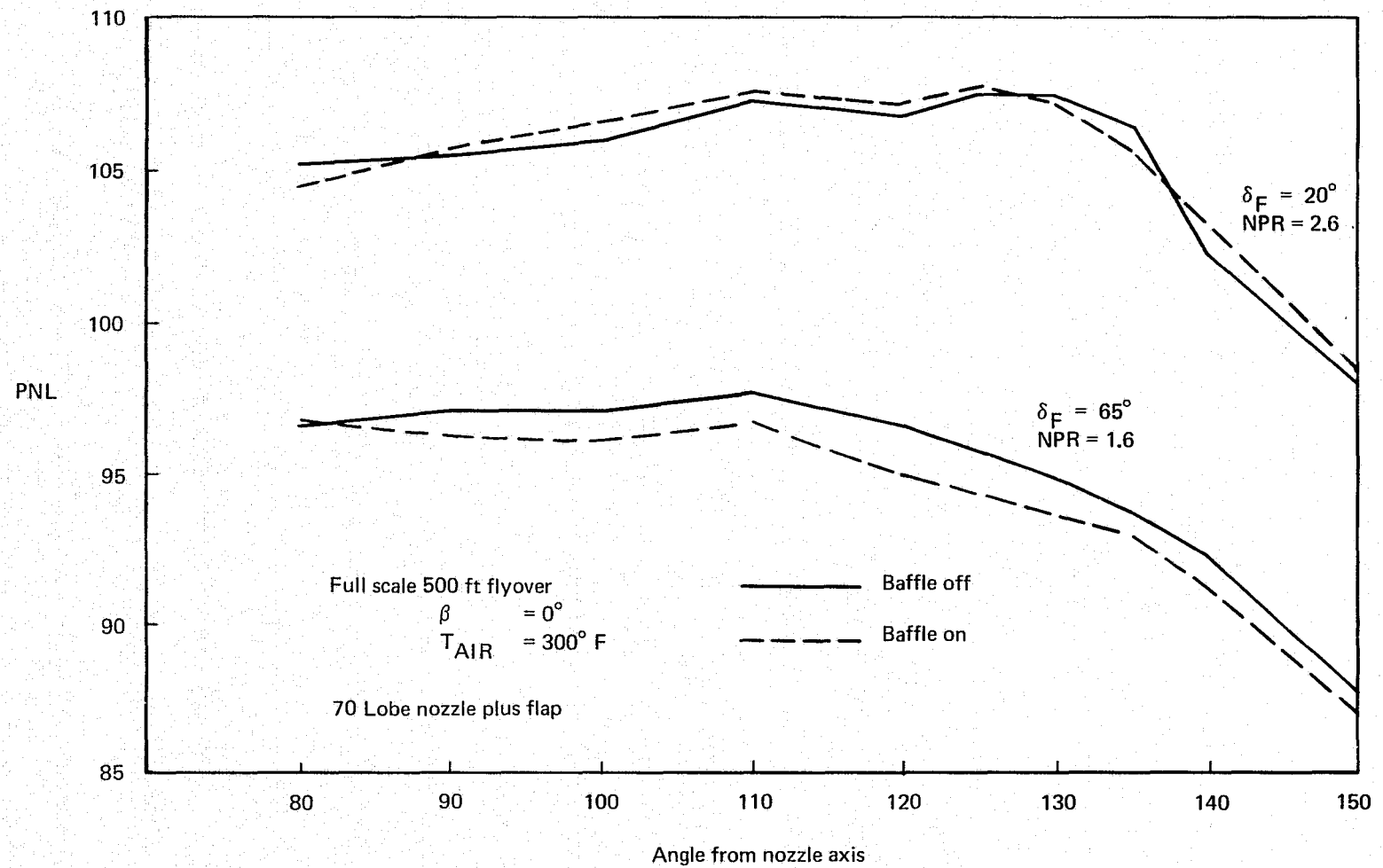

FIGURE 4.–EFFECT OF BAFFLE AT TAKEOFF AND APPROACH FLAP SETTINGS

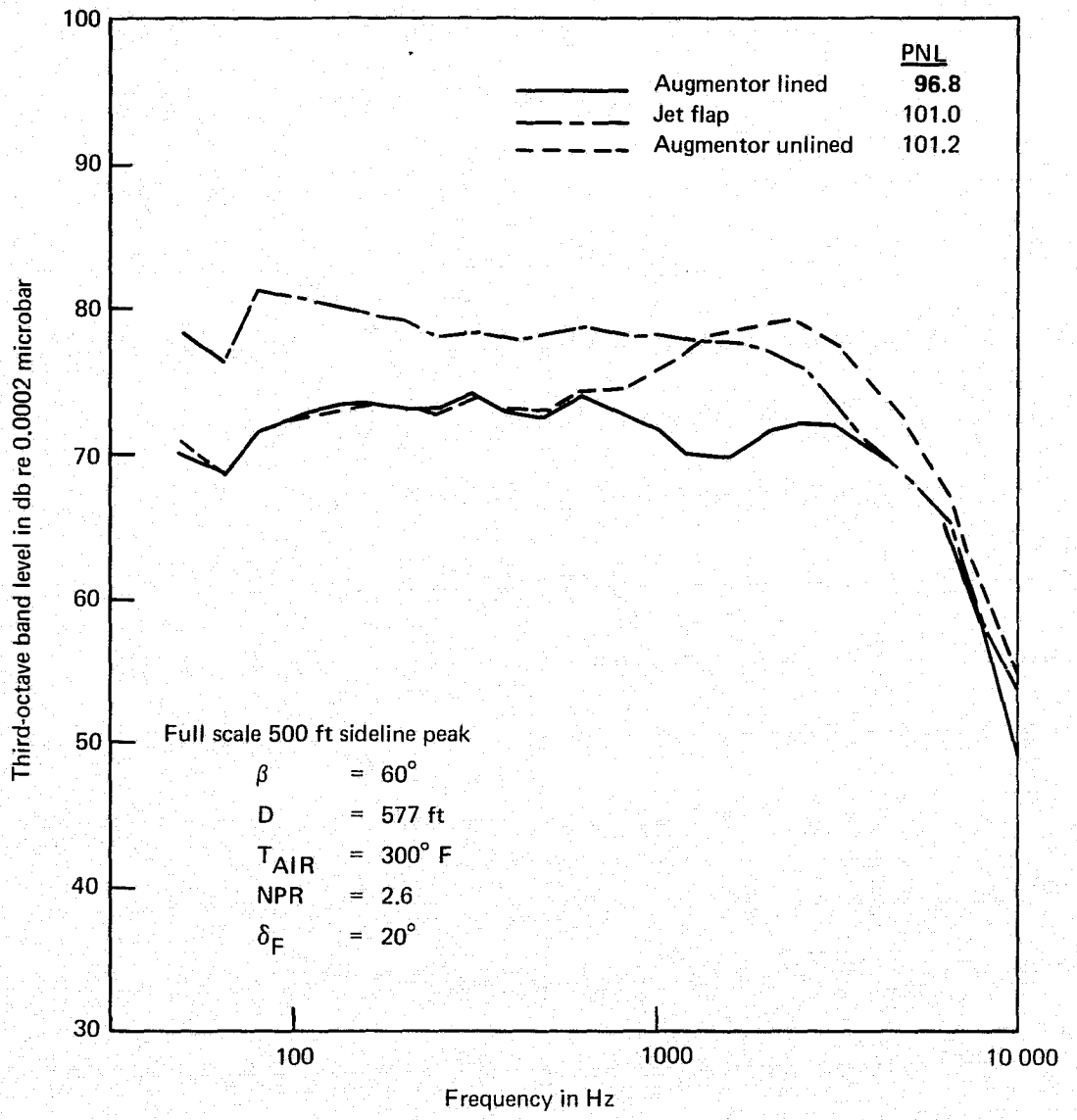

FIGURE 5.–COMPARISON OF JET FLAP AND AUGMENTOR NOISE (TAKEOFF)

jet flap produces considerably more low-frequency noise and less high-frequency noise than the unlined augmentor.

Figure 6 is a comparison of the noy-weighted spectra of the two powered-lift concepts. The peak perceived noise level of the jet flap is sharply dominated by noise at frequencies between 1250 and 4000 Hz, not by the low-frequency noise which appears to be dominant in figure 5. This indicates promise that the jet flap, too, could be acoustically modified to reduce its high-frequency peak. Modifications to the jet flap system for this purpose might involve corrugating the jet nozzles, treating the flap trailing edge, or improving the shielding properties of the flap configuration.

Before recording the noise levels produced by the nozzle and flap system, flow attachment on the flap upper surface was attained at each flap deflection angle tested. Nozzle-flap positions that produced the highest thrust levels while maintaining flow attachment were sought. The system thrust levels developed at both flap angles tested are shown in figure 7. The thrust ratio presented is the resultant thrust with the flap on divided by the thrust produced by the nozzle alone. At 20° flow turning some thrust augmentation is produced (1.03), while at $\delta_F = 65°$, the increases in jet flap impingement required for flow attachment reduce the thrust ratio to about 0.94. For low turning angles such as the takeoff case ($\delta_F = 20°$), a favorable static pressure gradient is created on the flap leading edge, which more than makes up for the losses due to flow impingement required for flow attachment.

The static flow turning performance for both turning angles tested is summarized in figure 8. The effects of Z position (closeness of the coanda surface to the jet flow) and nozzle air temperature are shown for $\delta_F = 20°$ and 65°. Flow attachment is indicated for all conditions shown as the effective turning angles (δ_J) are within a few degrees of the flap angle (δ_F). The data indicate that slightly higher turning angles are attained with heated air. Also, at the approach turning angle, more negative Z values were required to maintain flow attachment. As the flap angle is reduced, less flow impingement is required and the desired Z position is based on the position resulting in the highest thrust recovery. At the takeoff flap setting ($\delta_F = 20°$), a thrust recovery ratio over 1.0 is realized.

Flow attachment at a steep flap angle representing an approach condition was demonstrated here under static conditions. Further evaluations of this system would require demonstration of flow attachment under wind-on conditions.

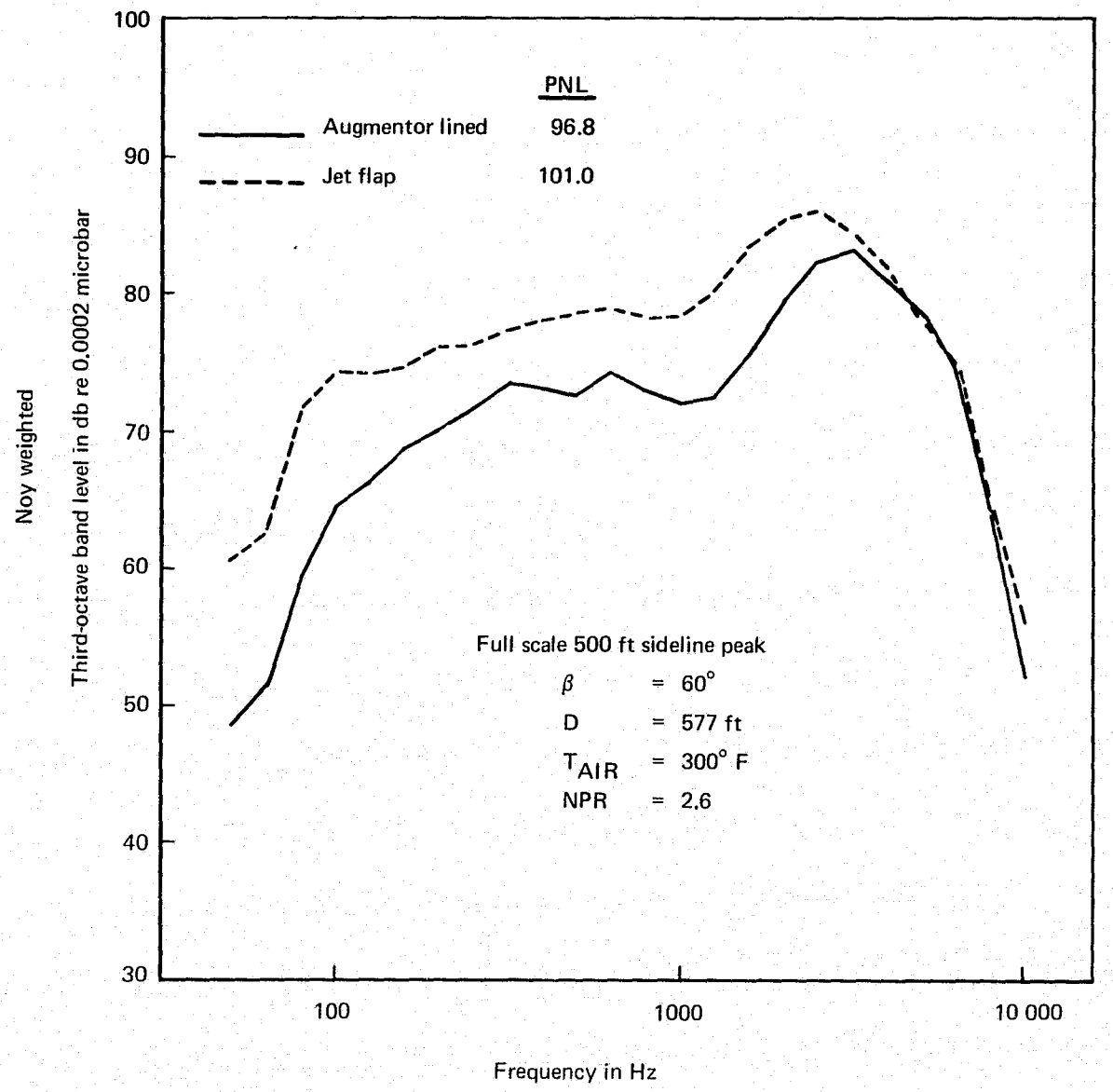

FIGURE 6.—NOY-WEIGHTED COMPARISON OF JET FLAP AND LINED AUGMENTOR

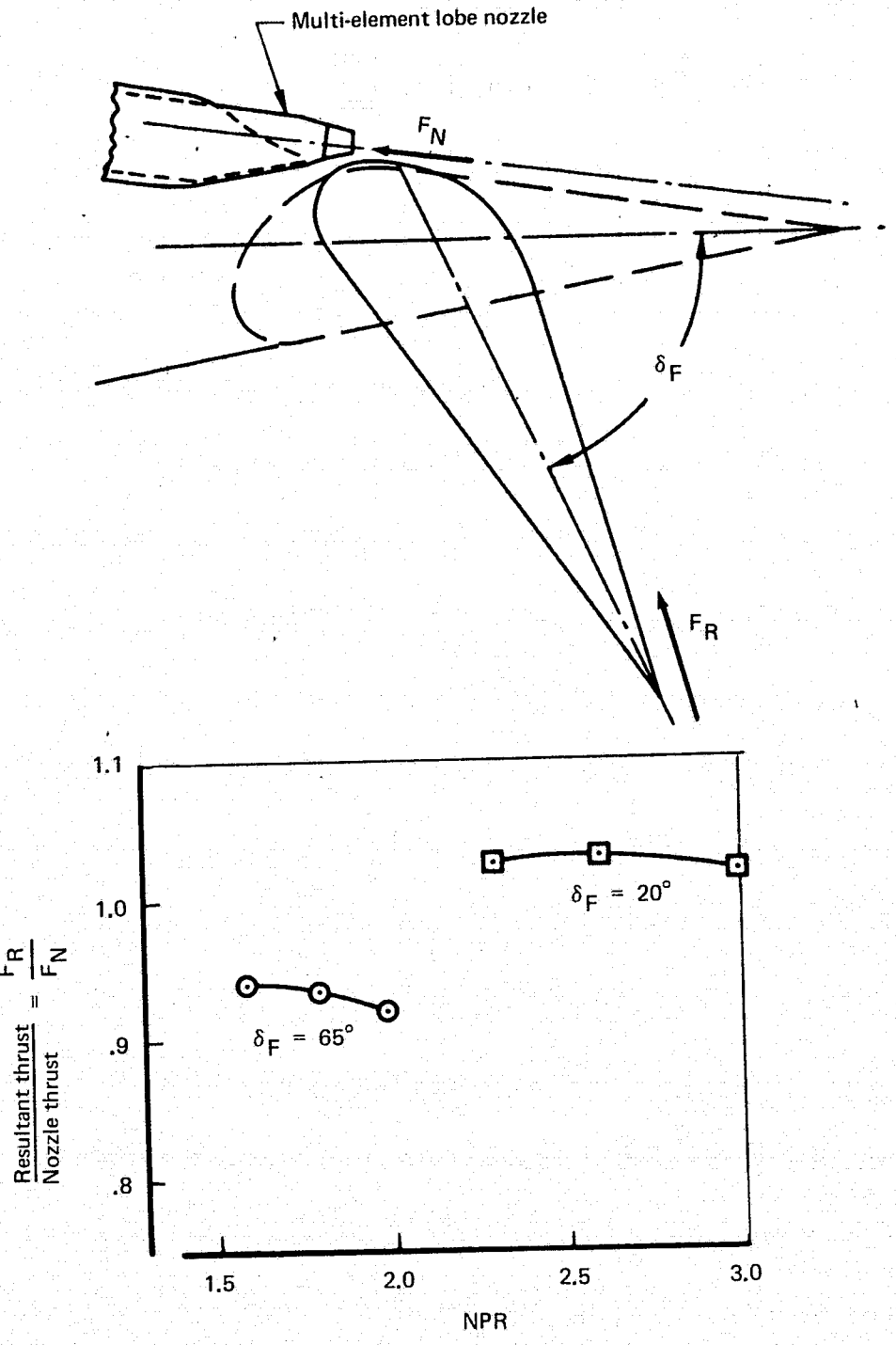

FIGURE 7.–JET FLAP MODEL–STATIC THRUST PERFORMANCE

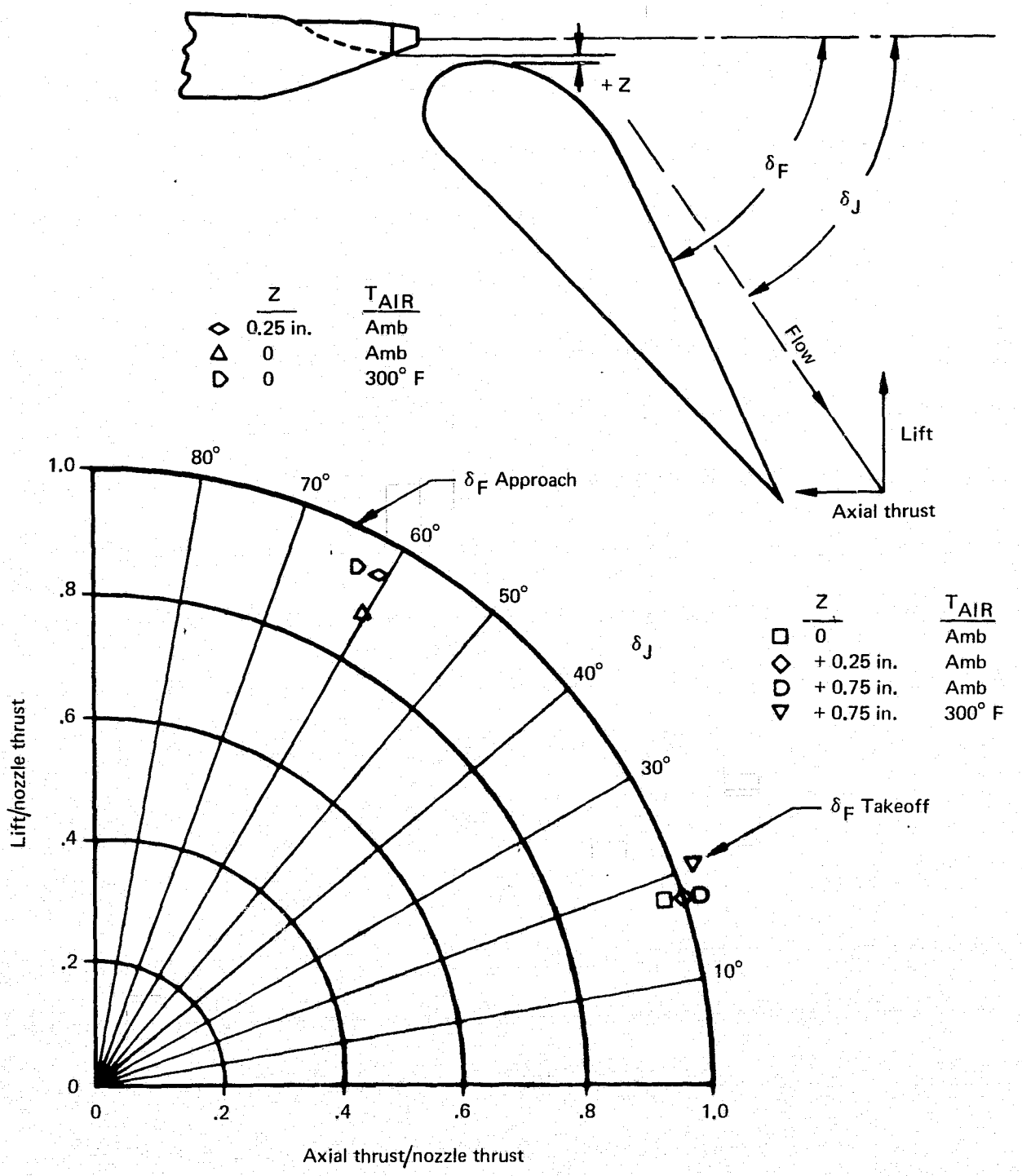

FIGURE 8.—JET FLAP MODEL STATIC TURNING PERFORMANCE

INTRODUCTION

The potential for application of the augmentor wing concept to commercial STOL airplanes is reported in references 1, 2, 3, 4, and 5. The referenced studies demonstrated by test that high levels of thrust augmentation and noise suppression could be achieved by use of high area ratio multi-element nozzles exhausting through an acoustically lined three-element augmentor flap. Although the designs showed that the augmentor flap could be stowed within a high-speed wing envelope, additional complexity and weight were indicated compared to more conventional systems.

During the referenced studies, a few noise tests were conducted with multi-element nozzles of low array area ratio* (2 to 4) and with the lower flap element only. The limited amount of data indicated that the single lower flap offered a significant amount of noise reduction through shielding. Reduced flow height in the same total flow span is expected to result in greater shielding of noise heard below the wing. The wing provides shielding of the noise propagated from sources at and near the jet nozzles (ref. 6, for example). Shielding will be greater for the low AAR (reduced height) nozzles because:

1. Higher acoustic frequencies are generated with reduced nozzle dimensions, and shielding is more efficient for higher-frequency, shorter-wavelength sound.

2. More shielding surface is available compared to the physical extent of noise source regions, and shielding improves with the ratio of flap length to nozzle height (ℓ/h).

At the same time, flow-upon-surface interaction noise is not expected to increase as ℓ/h increases beyond the situation where the jet core is shorter than the flap. It has been found that the potential core does not pass over the flap edge when ℓ/h is greater than eight (ref. 7).

Also, examination of the noise suppression characteristics of many multi-element suppressor nozzles tested indicated that breakup nozzles with small array area ratio (2 to 4) were superior in noise suppression to nozzles with higher array area ratios (6 to 8). Because of their high thrust augmentation characteristics, nozzles with high area ratios were desirable for use with an augmentor (ejector) flap and were selected for use in the final augmentor wing airplane designs.

Flow turning performance is directly related to the blowing nozzle height and the flap coanda radius. A favorable ratio of coanda radius to nozzle height is realized by using a suppressor nozzle of

*For a given blowing span, low array area ratio nozzles are nozzles small in height and approach a slot (AAR = 1) as a limit. (See fig. 9).

$$\text{Nozzle array area ratio} = \frac{\text{Dotted area}}{\text{Shaded area}} = \frac{\text{Nozzle area + secondary area}}{\text{Nozzle area}}$$

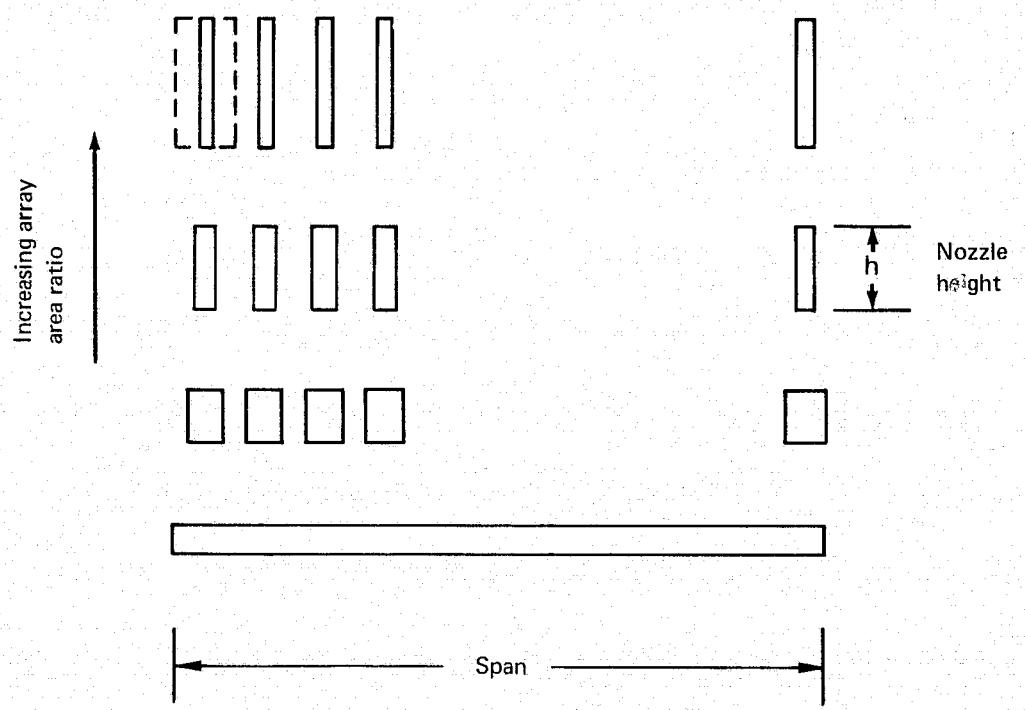

FIGURE 9.–DEFINITION OF NOZZLE ARRAY AREA RATIO

low array height in conjunction with a thick flap. Elimination of the shroud and intake door from the augmentor wing system provides an increase in the volume available for a flap with a larger coanda radius. Removal of these upper flap elements results in eliminating much of the complexity and weight inherent in the augmentor flap concept.

Potential application of a distributed blowing system with only a single element flap is strongly dependent on the noise suppression levels attainable by nozzle design and shielding from the flap. Demonstration of the noise suppression potential of this concept was accomplished by using an existing multilobe suppressor nozzle with an array area ratio of 2.7 and a new large radius flap sized to fit the wing geometry of the airplane described in reference 4. The results are reported in this document.

SYMBOLS AND ABBREVIATIONS

A	area, sq in.
A*	blowing nozzle area at Mach 1.0
AAR	augmentor primary nozzle array-area-ratio (ratio of the area bounded by the primary nozzle exits to the measured nozzle exit area)
AR	augmentor nozzle aspect ratio, b/h, or wing aspect ratio
BBL	body buttock line
b	augmentor span, in.
C	correction factor (as a function of frequency), dB, or wing chord, in.
C_D	nozzle discharge coefficient, measured airflow/ideal airflow.
C_F or ℓ	flap chord/wing chord, or flap chord, in.
C_V	nozzle velocity coefficient, measured thrust/(measured mass flow x ideal velocity)
D	diameter, in.
EGA	Extra ground attenuation
F_N	primary nozzle thrust
F_R	system resultant thrust
f	frequency, Hz
g	gravitational constant, ft/sec^2
Hz	Hertz, a unit meaning cycles per second
h	height, in., slot (or equivalent slot, $h_E = 0.432$ in.)

ℓ_Z	distance along a parallel to the nozzle centerline, in. (see fig. 17)
M	Mach number
m	airflow, slugs/sec (measured)
NPR	nozzle pressure ratio
OASPL	overall sound pressure level, dB
$OASPL_{max}$	maximum OASPL along a noise radiation line with respect to the jet axis
OBSPL	octave-band sound pressure level
PNdB	unit of perceived noise level
PNL	perceived noise level, in PNdB
PNL_{max}	maximum PNL along a noise radiation line with respect to the jet axis
q	dynamic pressure, lb/sq in.
R_c	coanda radius, in.
r	radius from nozzle exit to microphone or observer, ft
rh	relative humidity
S_N	Strouhal number (frequency x length)/velocity
SPL	sound pressure level in decibels (dB) re 0.0002 microbars
SR	slant range, ft
STOL	short takeoff and landing
T	temperature, °F
T/O	takeoff power setting

V	velocity, ft/sec
WCP	wing chord plane
w	lobe width, in.
Z	distance from coanda surface to a plane extended from nozzle lower surface (see fig. 17)
α	air absorption (as a function of frequency), dB/1000 ft
β	nozzle or flap orientation with respect to flyover position, deg (see figs. 11 and 23)
δ_F	flap rotation angle with respect to WCP, deg
δ_N	augmentor primary nozzle deflection angle with respect to WCP, deg
θ	noise radiation angle with respect to thrust vector, deg (see fig. 23)
λ	wavelength, m ft
ρ	jet density, lb/ft^3

DISCUSSION

TEST FACILITY AND MODEL DESCRIPTION

In the paragraphs that follow, details of the test facility, test procedures, and instrumentation are discussed, as well as the accuracy and repeatability of performance and acoustic measurements.

Facility

The Boeing North Field Acoustic Arena in Seattle, Washington, was chosen as the test location. This facility is especially suitable for large-scale combined acoustic and thrust performance test programs. Thrust is measured with a six-component, platform balance bridged with high-pressure air; the noise can be measured in a 180° arc in an acoustic arena as shown in figures 10 and 11. The thrust stand accurately measures model forces using either heated air at 300° F or ambient-temperature nozzle air. Nozzle flow rates are determined with precision using ASME venturi flowmeters calibrated against a Boeing standard nozzle. An acoustically treated muffler plenum, located on the balance platform upstream of the test nozzle plenum, prevents noise generated by the air supply lines and control valves from reaching the test nozzles.

To acquire acoustic data of the highest quality, data were recorded only during a limited range of atmospheric conditions. Because of the precision desired for acoustic measurements, each component of the instrumentation system for noise measurement was carefully chosen and integrated. The basic noise-measuring system consists of microphones, a tape recorder, and one-third octave band analysis instrumentation calibrated and operated over a frequency range of 200 to 40 000 Hz. The output is punched cards, which are used to make computer plots of one-third octave band level versus frequency and other calculations used in the analysis.

Data Repeatability

Performance

Before beginning the tests on the lobe nozzle and flap, a 100/1 AR slot nozzle (fig. 12), used as a reference nozzle in previous tests, was installed and tested to check the facility thrust and airflow measuring system after a period of inactivity. The slot nozzle performance data (velocity and discharge coefficients), measured just prior to beginning the jet flap tests, are shown plotted with data recorded during the Task VIIC of the Augmentor Wing Design Integration and Noise Studies (ref. 3) in figure 13.

FIGURE 10.—THRUST STAND AND ACOUSTIC ARENA

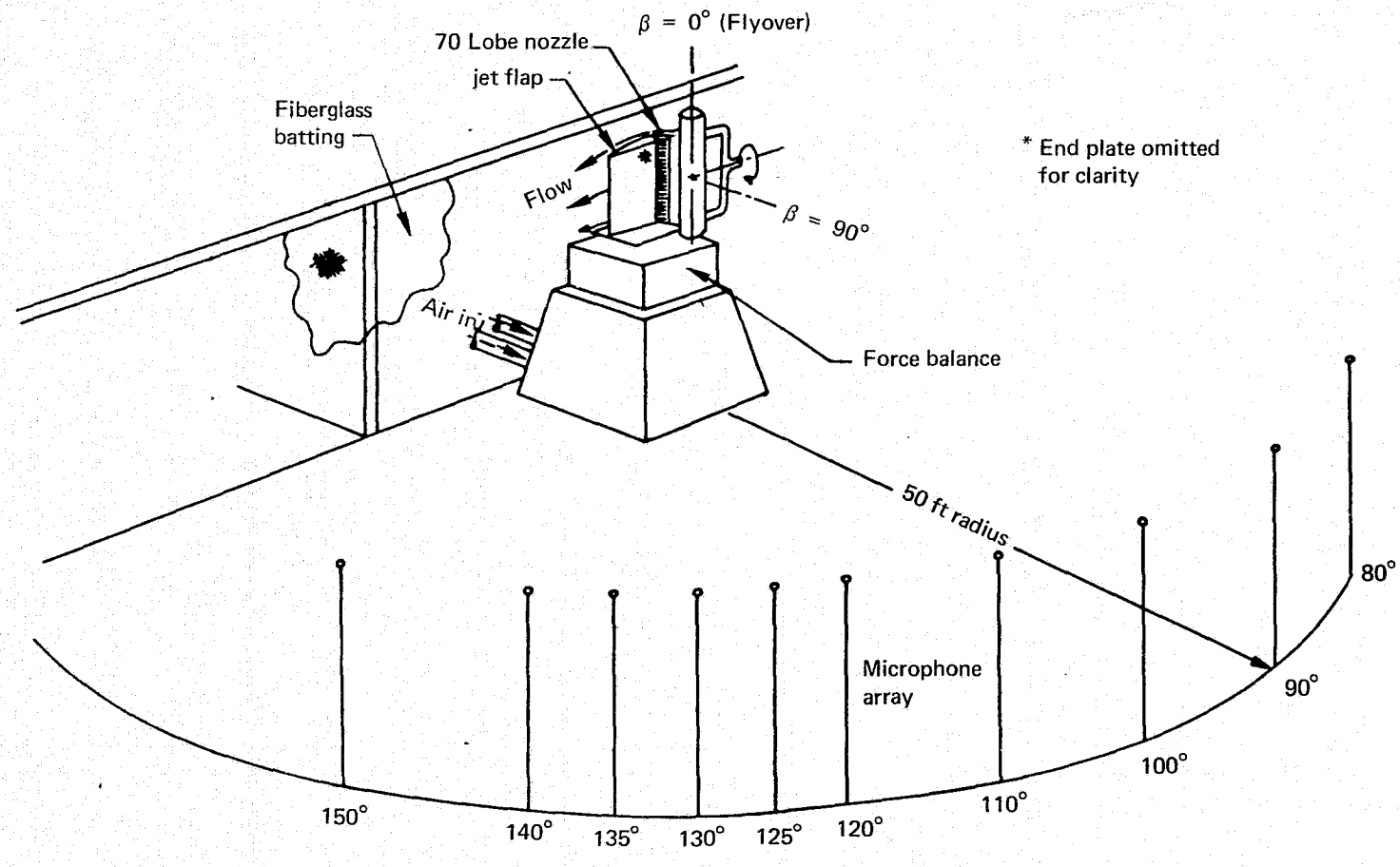

FIGURE 11.–MODEL INSTALLATION AND ACOUSTIC ARENA

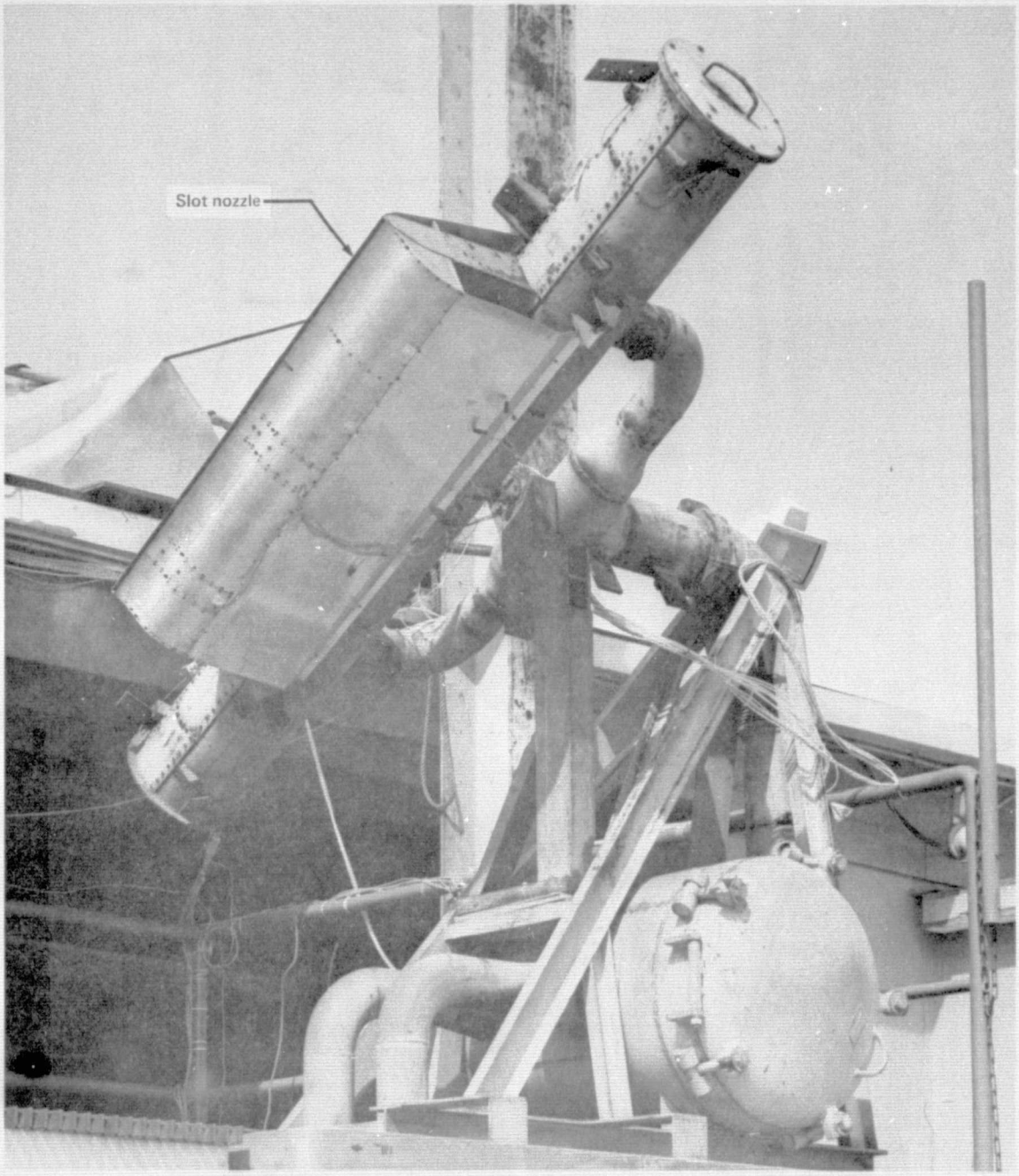

FIGURE 12.–REFERENCE NOZZLE–100:1 ASPECT RATIO SLOT

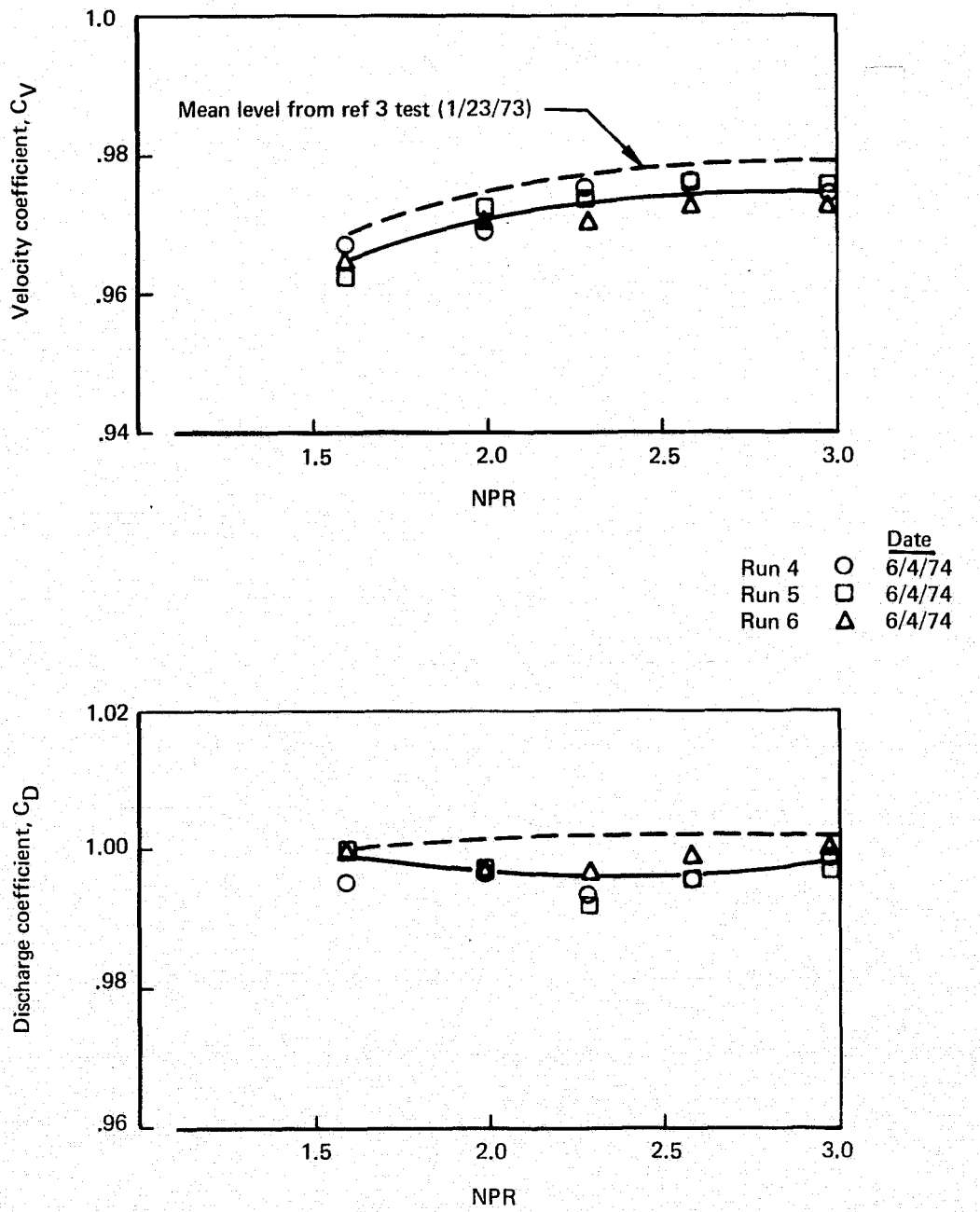

FIGURE 13.–SLOT REFERENCE NOZZLE PERFORMANCE REPEATABILITY

The reference slot nozzle performance data (runs 4 to 6) show good agreement with the performance levels measured nearly a year earlier. The discharge coefficient levels at or near 1.0 are not of concern, as some uncertainty exists in knowledge of the precise nozzle exit area.

The data from these four runs indicate a repeatability of test results of approximately ±0.5%. The balance lift axis (reverser vertical vector) was not used in the reference nozzle check runs but was calibrated by use of calibration weights.

Acoustics

It was anticipated that the newly obtained jet flap noise results would be directly compared to previously obtained data for various jet nozzle arrays and augmentor flap systems. To assure that these comparisons can be made—that nothing associated with the test facility, acoustic arena, or data acquistion system has changed significantly since the earlier tasks—a basic jet nozzle configuration was retested in the new test series. Representative results from the old and new noise measurements for this 100:1 aspect ratio slot nozzle are presented in figure 14. At both the nominal approach and takeoff jet velocities (nozzle pressure ratios of 1.6 and 2.6), there is the usual scatter of SPL results at the very low frequencies caused by uncorrectable variability in sound propagation over a ground plane and an increase of 1 to 2 dB with the new measurements in the frequency range from about 500 Hz to 1600 Hz. The latter spectral change is not readily explainable. There is no reason to think that the jet nozzle (sound source) has changed, so this small acoustic difference is attributed to factors in the arena geometry and properties of the air medium on test day. It is seen that the nozzle screech tone at 2000 Hz has been repeated almost exactly. Differences in peak sideline PNL are within 2 PNdB, with the new measurements being the higher.

Model Description

The nozzle selected for these tests was an existing multilobe suppressor nozzle built under NASA Contract NAS2-6344 Task I (ref. 5). The nozzle was the smallest array-area-ratio (2.7) multi-element nozzle built under this NASA contract. The nozzle was made up of 70 individual lobes of dimensions and spacing shown in figure 15. Jet screech control devices were not originally installed on the nozzle but were added for this program to eliminate the noise penalties associated with supercritical operation. The mechanism and control of supercritically related acoustic jet screech noise is discussed in references 1 and 2. An effective method of controlling jet screech noise (described in ref. 1) is to fit each lobe with a thin central splitter extending beyond the nozzle exit as shown in figures 15 and 16. The length of the splitter extension is governed by the maximum pressure ratio that screech control is required. In this case an extension length equal to three nozzle widths is required to control screech noise up to a pressure ratio of 3.0. The trailing edge of the splitters is sharpened to minimize drag and to reduce the possibility of producing edge tones.

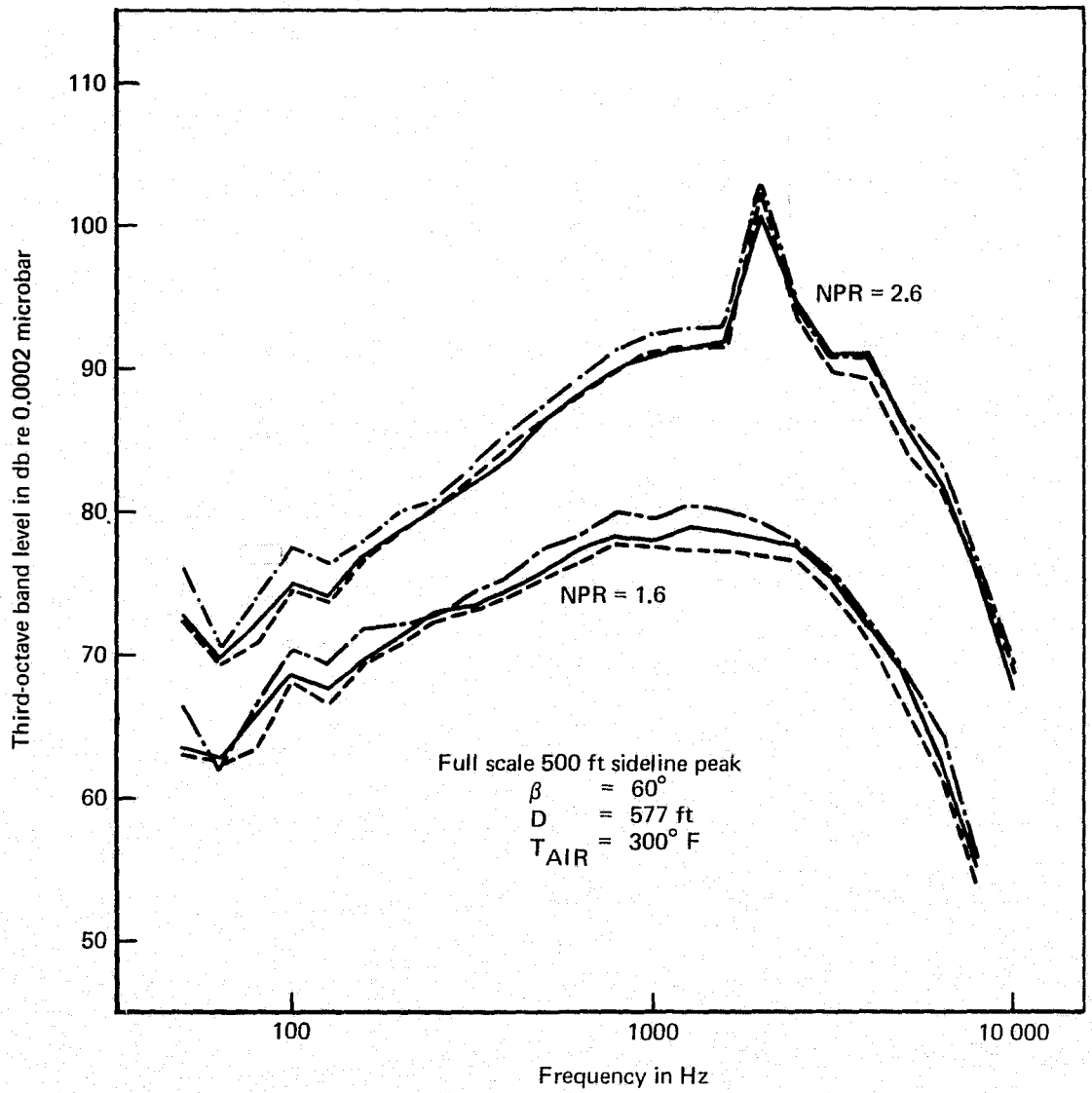

Reference nozzle—100/1 aspect ratio slot

		Ref	Date	PNL (1.6)	PNL (2.6)
———	Run 1601	2	6/30/72	99.9	117.1
– – – –	Run 2018	1	9/1/72	99.0	117.7
—·—·—	Run 30		6/7/74	100.6	118.5

FIGURE 14 –SLOT REFERENCE NOZZLE NOISE REPEATABILITY

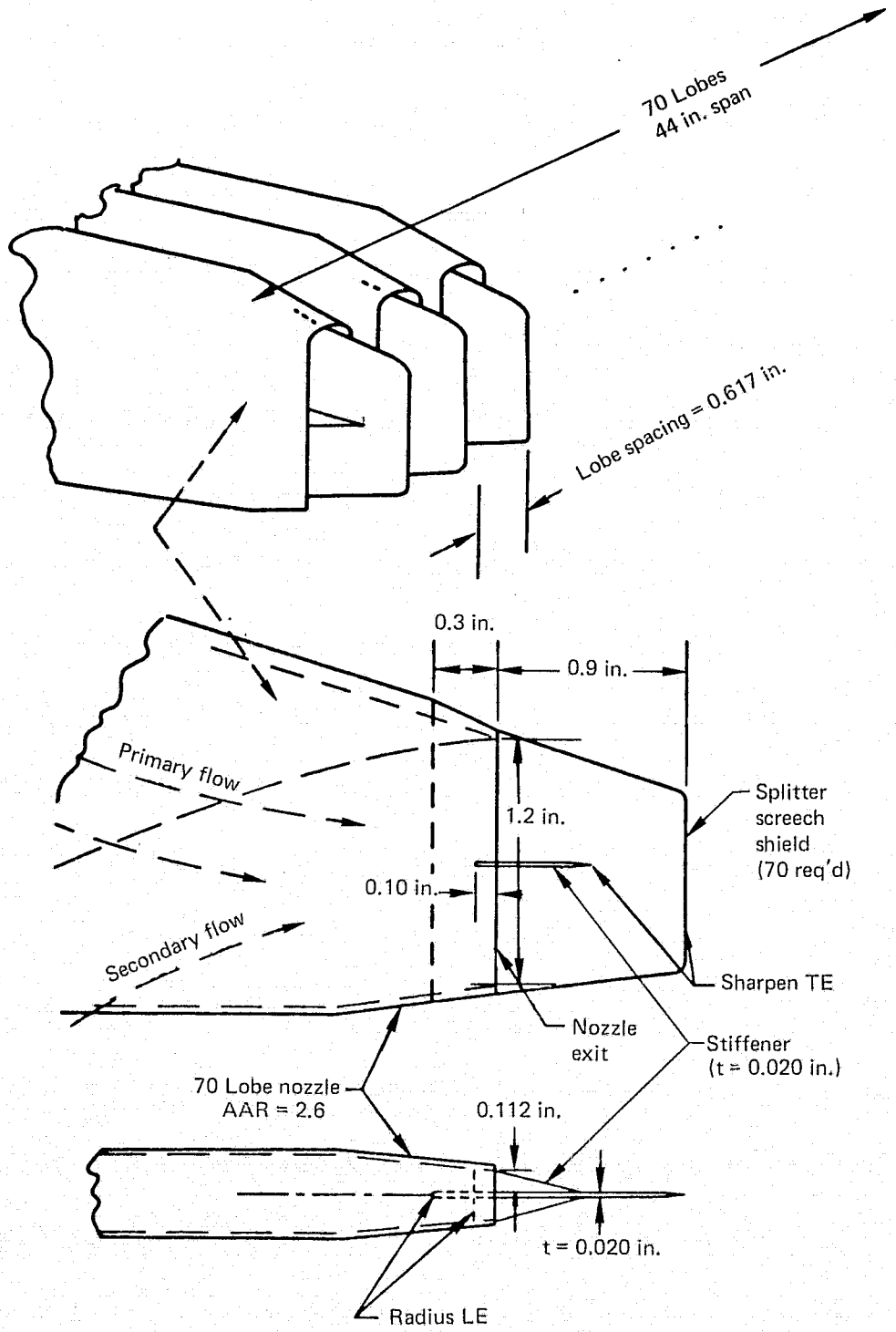

FIGURE 15.—70 LOBE NOZZLE DESIGN WITH SPLITTER SCREECH SHIELDS

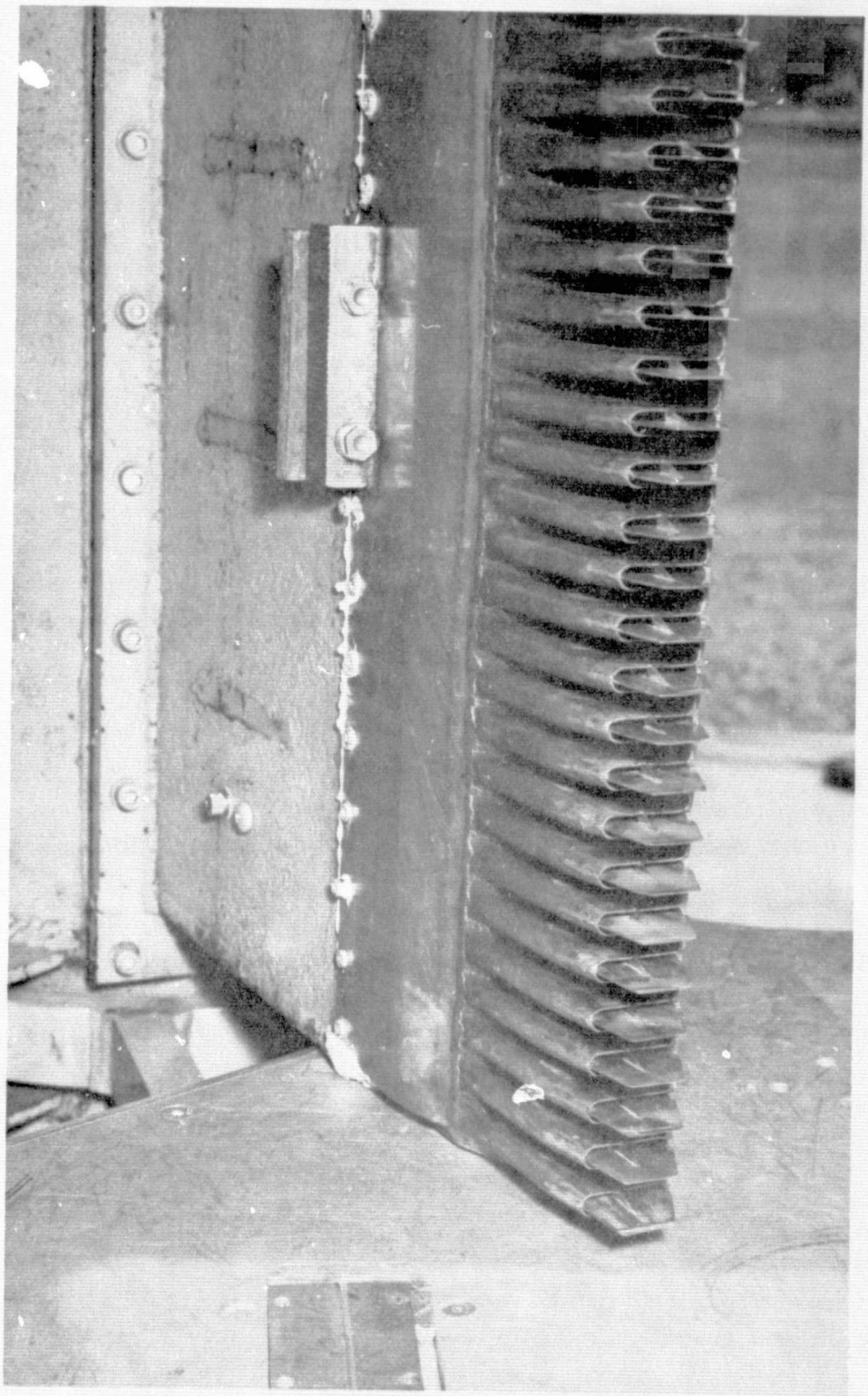

FIGURE 16.—70 LOBE NOZZLE WITH
SPLITTER SCREECH SHIELDS

The flap was designed to fill the space available in the wing trailing edge as shown in figure 17. It is of wood construction and is defined in figure 18. The test installation showing the nozzle, flap, and end plates is pictured in figures 19 and 20.

In order to evaluate the effect of noise leakage through the lower nozzle-flap gap, the flyover noise data ($\beta = 0°$) were recorded with and without the gap covered for both takeoff and approach flap settings. The gap was covered by a sheet metal baffle as shown in figure 21.

Test Procedures

Before recording noise data with the flap installed, flow attachment at both turning angles (20° and 65°) was attained. Flow attachment is strongly influenced by the distance between the nozzle jet and the flap coanda surface. This distance is known here as the Z position (see fig. 17). Generally, as the flap deflection or turning angle is increased, the flap coanda surface must be positioned closer to the jet (increasingly negative Z), and at very steep angles the flow must strongly impinge on the flap surface. Flow attachment was indicated by determining the effective flow turning angle from the two measured thrust components. Flow attachment was assumed when the effective turning angle was within a few degrees of the flap deflection angle.

For both turning angles tested, several variations in Z position were tested with a constant longitudinal position ℓ_Z (see fig. 17) that was selected from previous experience. Nozzle pressure ratios associated with takeoff conditions (2.3, 2.6, 3.0) were set for the takeoff flap setting, and pressure ratios of 1.6, 1.8, and 2.0 were used for the approach flap settings. All acoustic data were recorded with the nozzle total and temperature equal to 300° F.

Noise data representative of different airplane/microphone orientations were obtained by rotating the flap and nozzle assembly with respect to the fixed 12-ft-high microphones as shown in figure 11. This angle of rotation is known as the Beta angle with $\beta = 0°$ and 90° representing flyover and sideline orientations, respectively. Acoustic data were also recorded at one intermediate position ($\beta = 60°$) for sideline directivity effects.

Performance Definitions

Nozzle Performance

Velocity coefficient, $C_V = F_N/mV_I = F_N/C_D m_I V_I$

Discharge coefficient, $C_D = m/m_I$

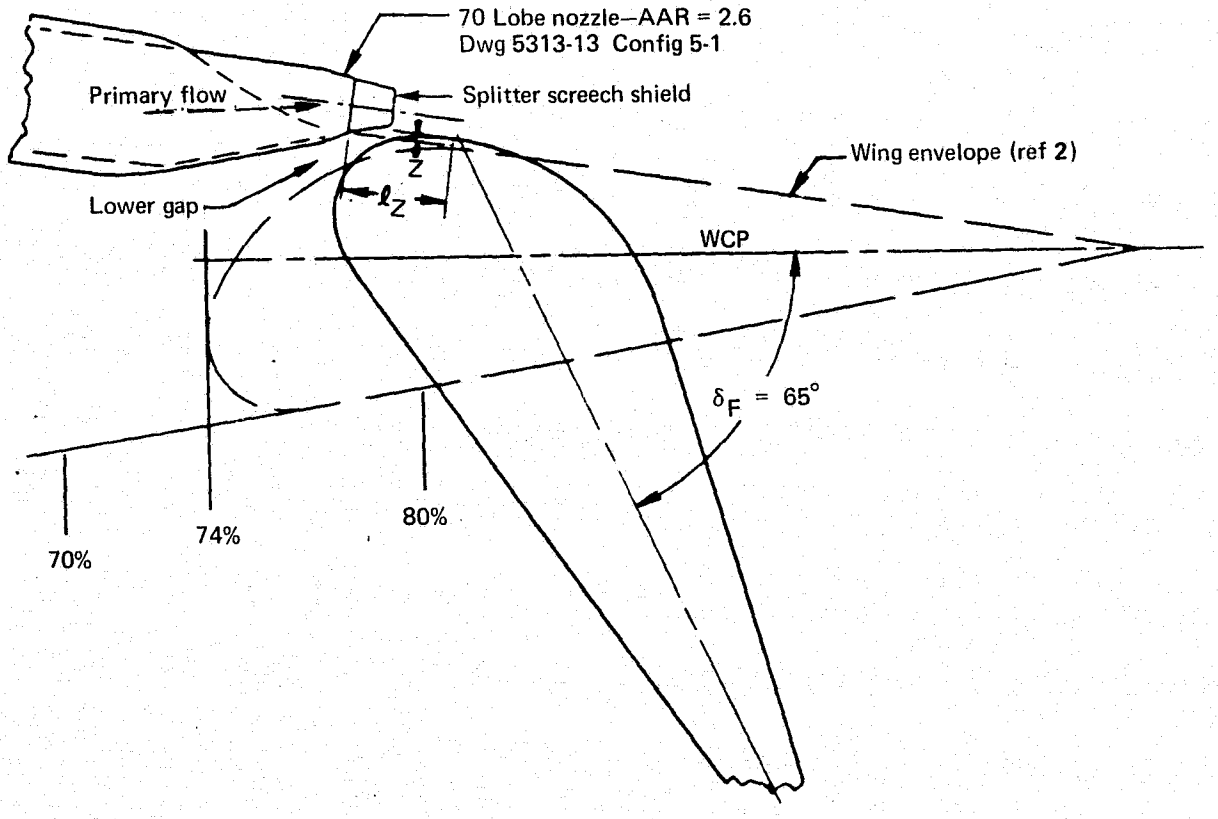

FIGURE 17.–JET FLAP INSTALLATION

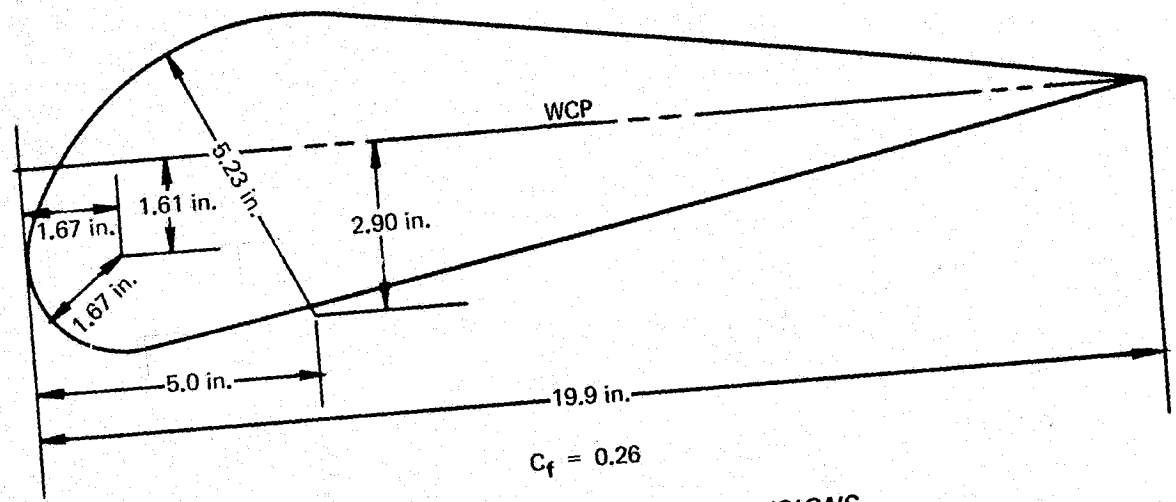

FIGURE 18.—JET FLAP MODEL DIMENSIONS

FIGURE 19.–JET FLAP MODEL INSTALLATION, $\delta_F = 20°$

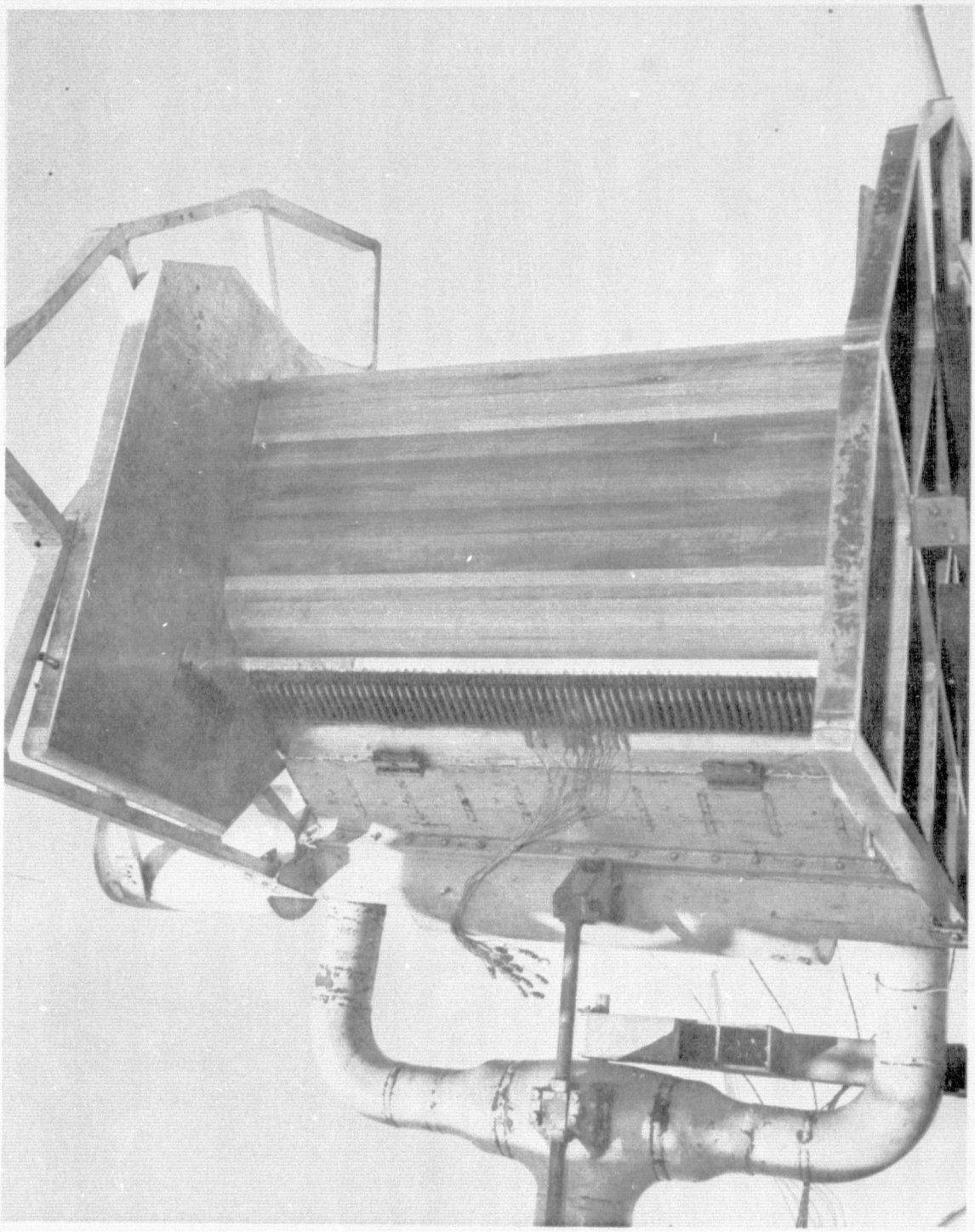

FIGURE 20.–JET FLAP MODEL INSTALLATION, $\delta_F = 65°$

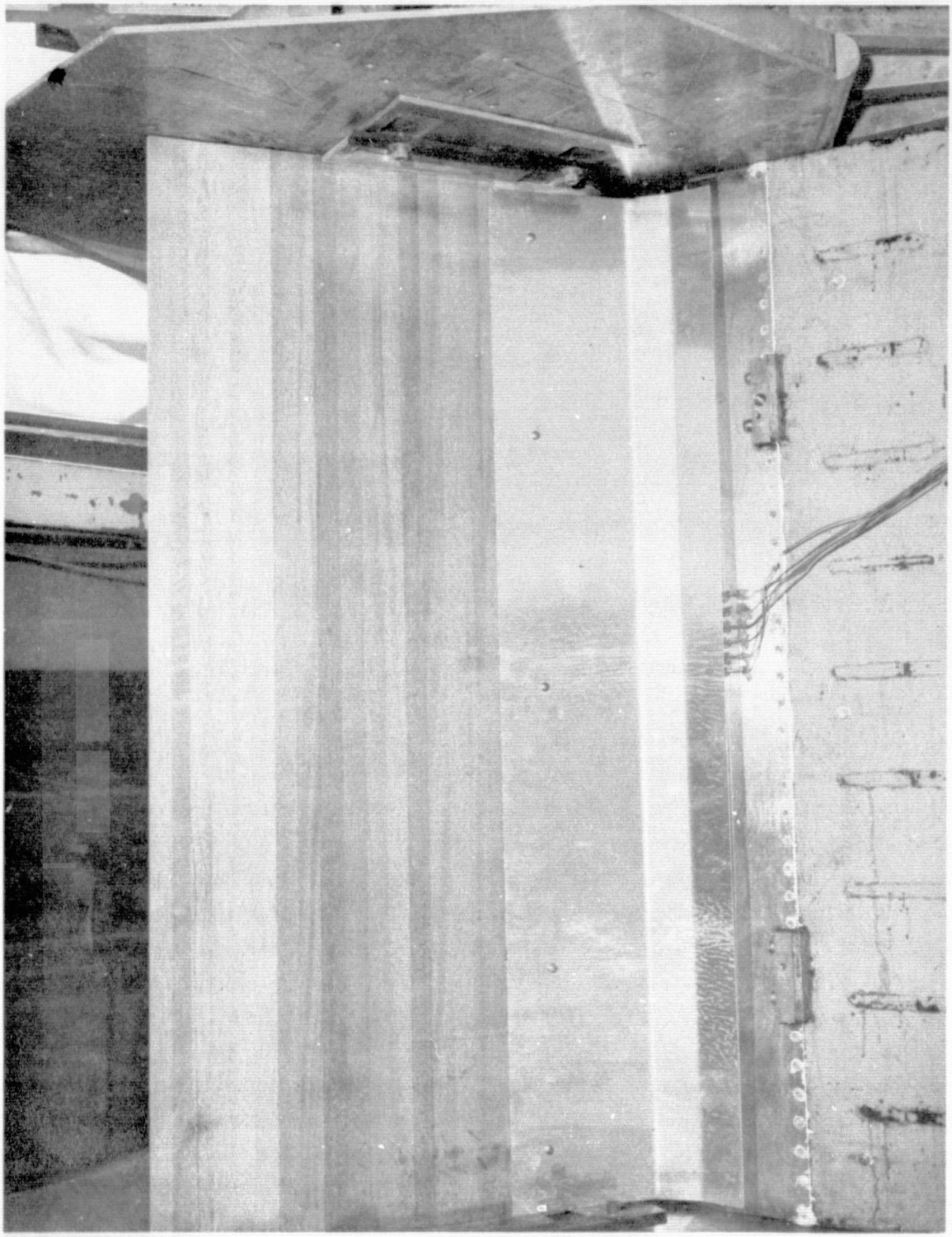

FIGURE 21.—JET FLAP MODEL WITH SHEET METAL ACOUSTIC BAFFLE

System Performance

Thrust Recovery = F_R/F_N

Jet turning angle δ_J = arc cos F_H/F_R degrees where

F_N = measured nozzle thrust, lb

m = measured nozzle mass flow, slugs/sec

V_I = isentropic velocity, ft/sec

m_I = ideal nozzle mass flow, slugs/sec

F_R = resultant thrust, lb

F_H = horizontal thrust component, lb

F_V = vertical thrust component, lb

Acoustic Scaling and Noise Extrapolation Procedures

Acoustic scaling follows aerodynamic noise source theory, which says that the total acoustic power radiated from a jet is proportional to flow density and to the second power of a characteristic flow dimension, and is a function of the flow velocity. For jet noise. the theory developed by M. J. Lighthill says that noise intensity is proportional to the eighth power of jet velocity and to the jet cross-sectional area (that is, to the second power of jet diameter). In these model tests, both the density and jet velocity (temperature and pressure ratio) of the model were kept identical to the full-scale prototype; only the characteristic dimension was scaled. For linear arrays of nozzles, this characteristic dimension is the effective height of the array. For the data presented in this report the ratio of full-scale to model effective height is taken as four to one.

The steps used to scale and extrapolate the noise measured from the jet flap scale models to a full-scale airplane installation are given in figure 22. In the first step, each acoustic measurement is reduced to 24 one-third octave-band sound pressure levels in the frequency range indicated. The spectra were measured on a 50 ft radius sphere at a number of positions chosen to include all probable directions from the airplane to the sideline and flyover observer locations.

Reduce model test data

1/3-octave band sound pressure levels

$r = 50$ ft $\quad h_E = 0.43$ in.

$f = 200$ to 40 000 Hz

Step 1

Scale data to aircraft effective nozzle height

Multiply all dimensions by scale factor (SF)

$SF = 4.0 \quad r = 200$ ft

$h_E = 1.72$ in.

$b = 172$ in.

$f = 50$ to 10 000 Hz

Step 2

Correct spectra to standard day (59° F and 70% RH)

Add factor (C_{SD}) to each 1/3-octave band level

$$C_{SD} = \left[\alpha(f)_{SD} \frac{200 \text{ ft}}{1000 \text{ ft}} - \alpha(f)_{meas} \frac{200 \text{ ft}}{1000 \text{ ft}}\right] \text{dB}$$

($\alpha(f)$ from SAE ARP 866)

Step 3

Extrapolate to observer position

Add factor (C_X) to each 1/3-octave band level

$$C_X = \left[-20 \log \frac{R}{200} - \alpha(f)_{SD} \frac{R-200}{1000}\right] \text{dB}$$

Step 4

Calculate perceived noise level at observer position

$$PNL = \left[33.2 \log (0.15 \Sigma N + 0.85 N_{max}) + 40\right] \text{PNdB}$$

Step 5

Span adjustment

Add factor (C_b) to perceived noise level

$C_b = 10 \log (b_{AIRPLANE}/b)$

$b_{AIRPLANE} = 866$ in.

$b = 172$ in.

Step 6

Adjust for relative velocity effects

Add factor (C_{RV}) to perceived noise level

$$C_{RV} = 60 \log \left[\frac{V_J - V}{V_J}\right]$$

Step 7

FIGURE 22.—STEPS USED IN SCALING AND EXTRAPOLATION OF NOISE

Scaling is performed as the second step. It consists of multiplying all linear dimensions by the scale factor. Using a scale factor of four, the 50 ft sphere becomes a 200 ft sphere, the effective nozzle height becomes 1.72 in., the span of the test section becomes 172 in., and the frequency range becomes 50 Hz to 10 kHz.

Corrections are applied to adjust the measured spectra (at 50 ft) or air absorption so that the adjusted spectra are as observed on a standard day. A different absorption value is applied to each frequency band. The correction to standard day atmospheric absorption is made as the third step in the extrapolation procedure.

The resulting full-scale noise at 200 ft is extrapolated to an observer at some other distance in step 4. The inverse square law is applied to all 24 one-third octave band levels, and an individual correction for air absorption is applied in each frequency band. The perceived noise level is calculated at the observer position in step 5.

Since the actual span of the full-scale aircraft nozzle system is 433 in. in each wing, a source area correction to take this into account is made in step 6. The correction for relative velocity, step 7, is made on the (demonstrated) assumption that jet flap noise levels follow relative jet velocity to the sixth power.

No attempt was made to account for the possible effects on observed full-scale noise due to extra ground attenuation (EGA). These effects are not well understood nor predictable through data "correction." EGA could be important in observed noise at sideline locations where the sound transmission path is close to the ground plane.

The observer position with respect to the airplane is illustrated in figure 23. Spherical coordinates are used to define a cone whose axis is in the same plane as the thrust axis of the jet flap system, with the vertex of the cone on the airplane's axis opposite the geometric center of the nozzle exit plane. The axis intersects the ground plane at an angle determined by flight attitude and flap deflection angle.

The three variables that define the observer position are:

- The distance, r, along the element of the cone passing through the observer position
- The cone half-angle, θ, measured from the forward projection of the flap thrust axis
- The rotation angle, β, measured about the vertical plane (body buttock line (BBL) = 0) beneath the airplane, to the observer position

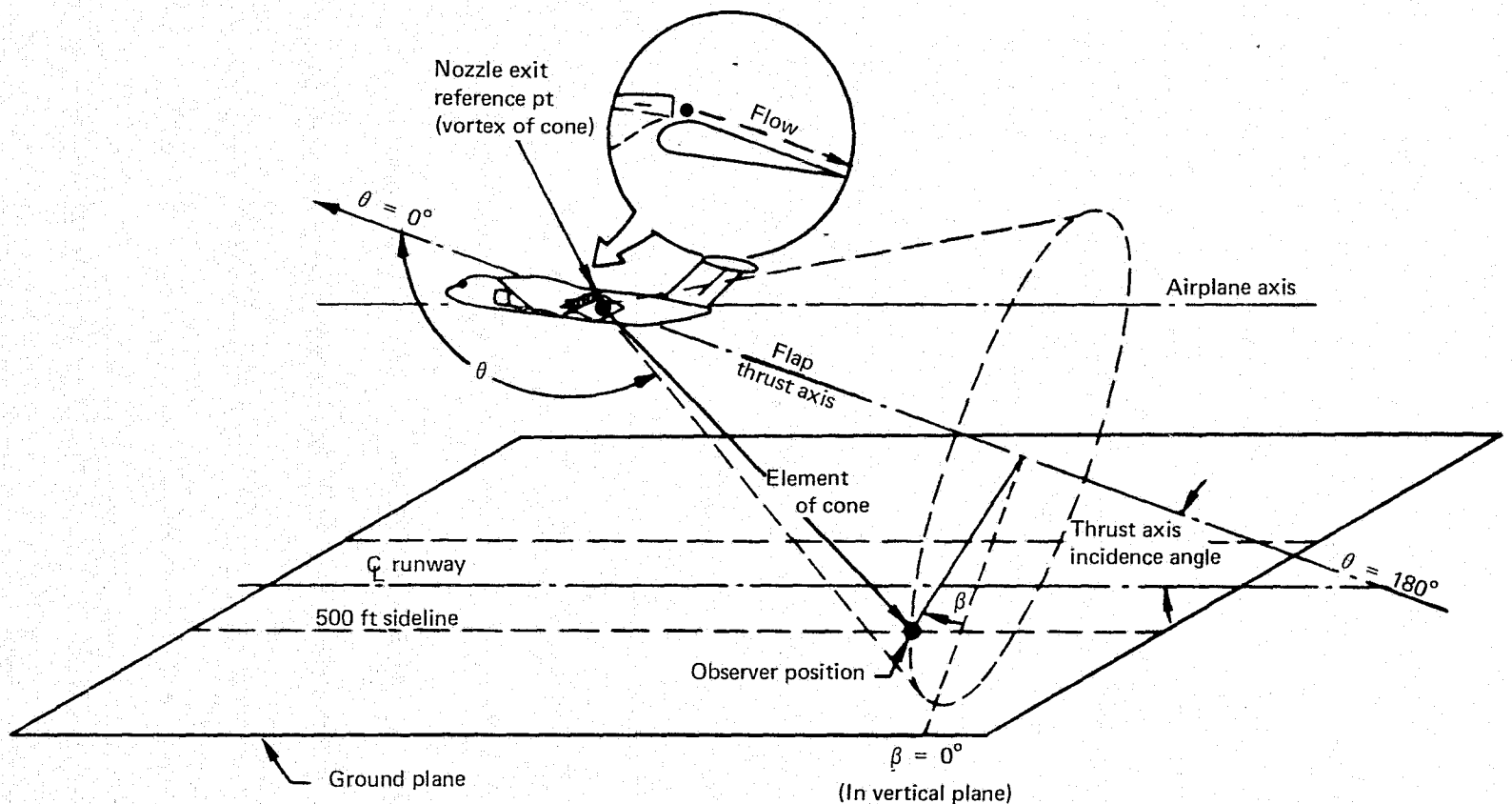

FIGURE 23.—COORDINATE SYSTEM TO RELATE OBSERVER POSITION TO JET FLAP NOISE SOURCES

The plane, defined by $\beta = 90°$ and the flap thrust axis, is parallel to, and is assumed to lie upon, the upper surface of the flap. Flyover noise is measured in the plane defined by $\beta = 0°$.

RESULTS

Acoustics

Noise of Nozzle Alone

The 70-lobe, AAR 2.7 nozzle was selected for use with the jet flap because of earlier results from noise testing of several jet nozzle configurations (see the Introduction). The previous tests of this particular nozzle configuration were done with an ambient temperature jet air supply, and the screech shield splitters were not installed at that time.

Figure 24 shows peak noise spectra of the multi-element nozzle measured in the previous tests compared with ambient temperature jet runs in the present test series. Excellent repeatability is evident particularly at the low jet velocity (NPR = 1.6). As jet velocity increased, there was increasing difference between the high-frequency levels. The original nozzle without splitter screech shields apparently did have additional high-frequency noise production. This noise was produced in broadband from (scaled) 500 Hz to 10 000 Hz in narrowly spaced tones less than one-third octave apart. The modified nozzle demonstrated greatly reduced high-frequency levels at the supercritical nozzle pressure ratios, indicating that the splitter did weaken the acoustic feedback mechanism causing screech. The lobed suppressor nozzle used with the jet flap was significantly quieter because of these splitters (ref. 1).

Figure 25 presents the hot jet peak noise results. The nozzle array produced a smooth, characteristically humped jet noise spectrum. As would be expected from multilobe breakup of the exhaust into many small jets there is a good deal of high-frequency content. The spectral valleys and peaks at very low frequency are typical of the measured data and appear to be slightly different in character for the various microphones in the polar array. The perceived noise levels for these spectra are calculated to follow a fifth power relationship on jet velocity over the entire tested velocity range; not the eighth power relationship typical of high-velocity jet noise from circular nozzles. It may be that presence of the screech shield splitters gave rise to a dominant jet/body interaction noise, which would be expected to vary as the fifth or sixth power of flow velocity.

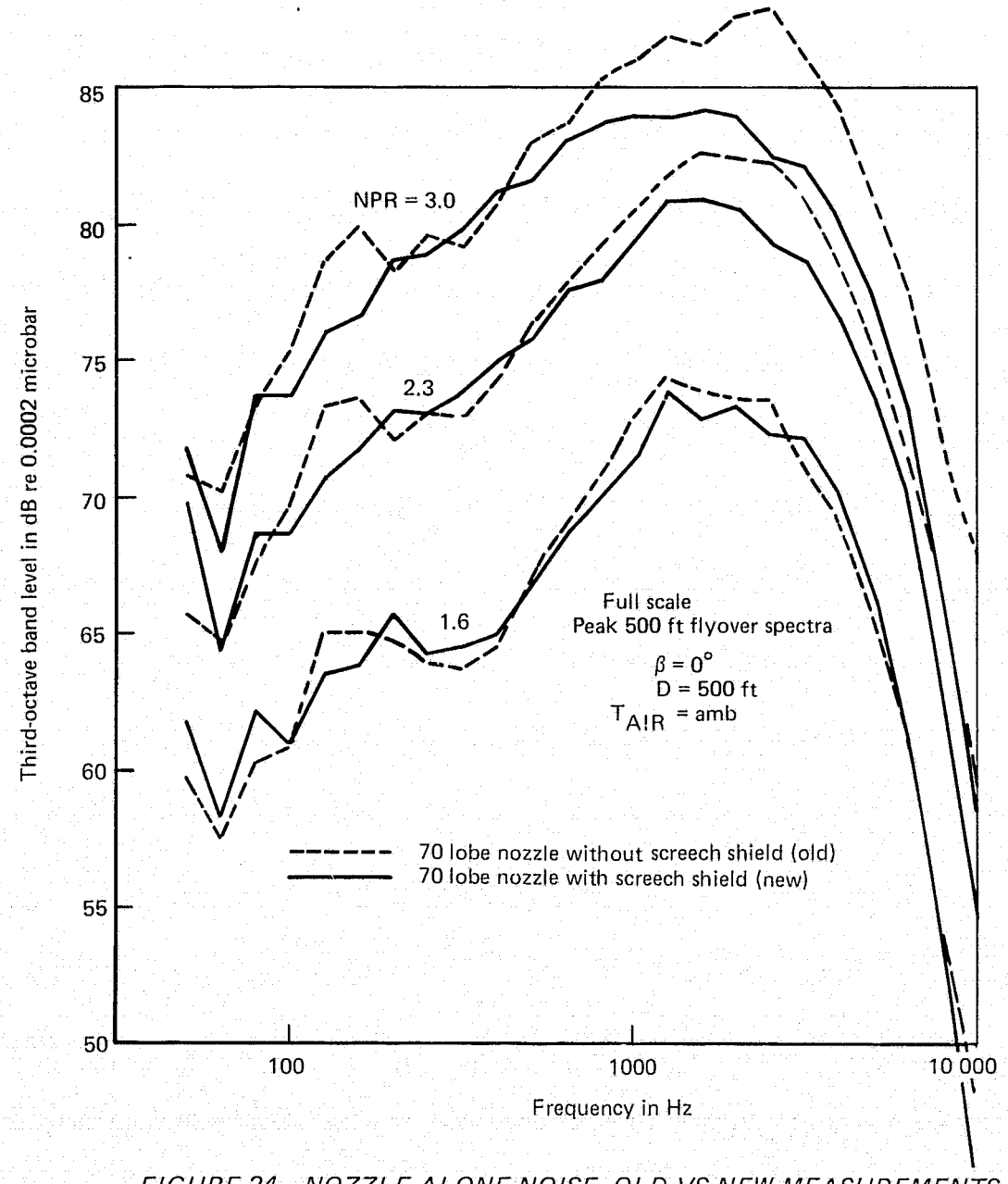

FIGURE 24.—NOZZLE ALONE NOISE, OLD VS NEW MEASUREMENTS

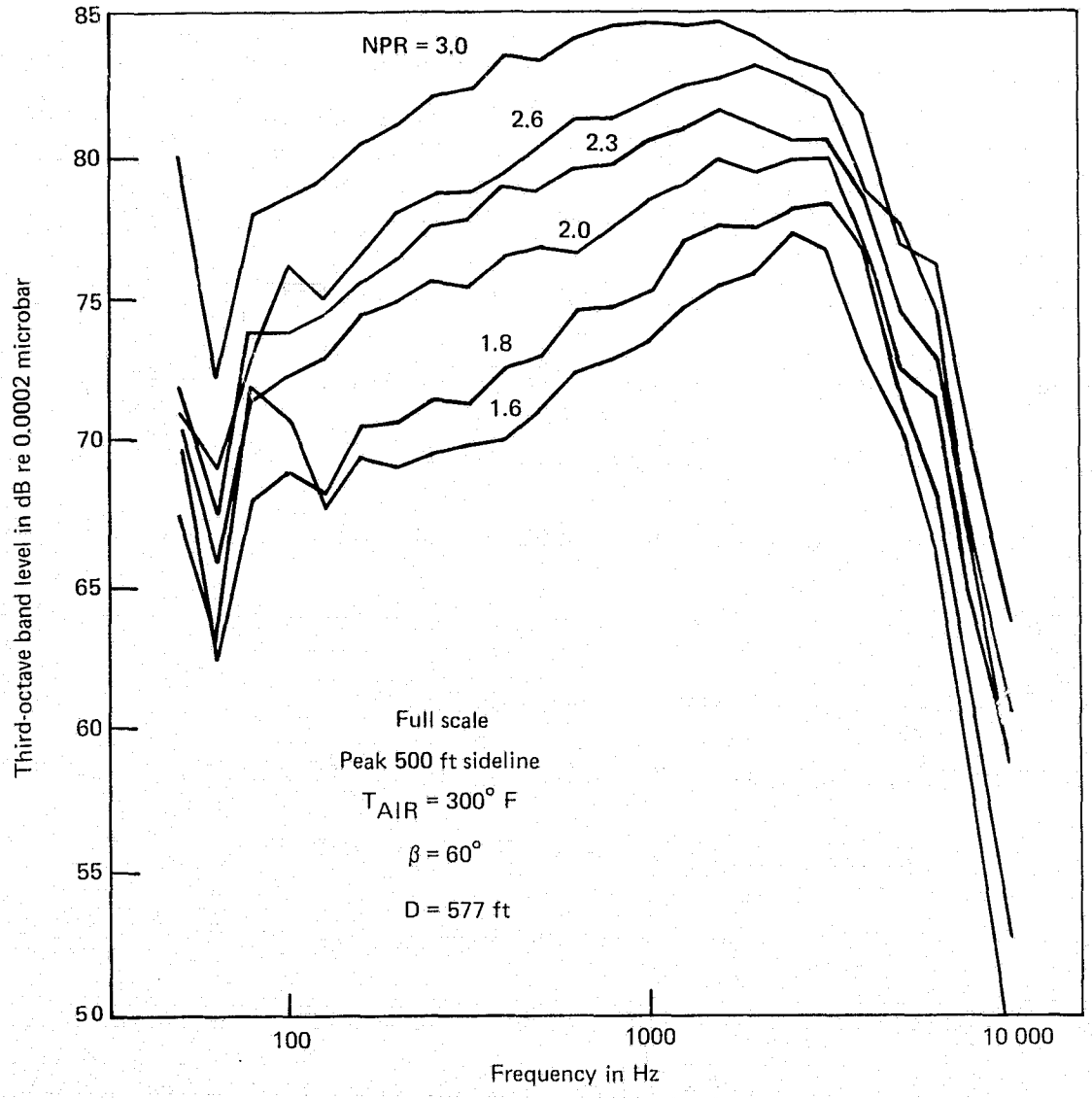

FIGURE 25.—NOISE OF 70-LOBE NOZZLE ALONE (WITH SCREECH SHIELDS)

Noise of Nozzle Plus Jet Flap

The peak noise spectra of the jet flap system at the two flap settings tested are presented in figures 26 and 27. Because of the effects of jet flap interaction and shielding, the smooth, single-humped spectrum of the jet nozzle system has changed into a double-humped spectrum shape with greater low-frequency content. Perceived noise levels of the jet-plus-flap system are found to be related to the eighth power of jet velocity at the 20° flap deflection angle (higher jet velocities) and to the fourth power at the 65° angle (lower jet velocities).

Acoustic behavior of the jet flap is illustrated by the flap on, flap off comparisons in figures 28 and 29. In both the nominal takeoff and approach configurations, the jet flap exhibits a shielding of high-frequency jet noise from the sideline observer to the extent of several decibels in certain one-third octave bands. The flap appears to be more efficient as a shield at the 20° deflection angle. This is a reasonable result, since the projected area of the shielding flap seen by the observer is reduced as the flap deflection angle increases.

The flap introduces a low-frequency noise source attributable to jet-flap interaction. Acoustic sources are related to jet turbulence impinging and scrubbing on the flap surface, and perhaps to edge effects when the turbulent jet passes over the sudden discontinuity from bounded to free flow at the flap trailing edge. As would be expected from the theory relative to acoustic efficiency of a turbulence interaction with surfaces and edges, the interaction noise introduced at low frequencies is markedly greater for the high jet velocity (takeoff) jet flap configuration.

The peak noise at the sideline was reduced more than 4 PNdB by addition of the jet flap (scaled to full size). This was true for both the takeoff and approach configurations.

Figure 30 shows that directivity patterns were not significantly distorted by the flap and that improvement in noise for the jet flap compared to the nozzle alone was experienced at all directivity angles. At the approach setting, although peak-to-peak noise improvement was 4 PNdB, the improvement at some off-peak times during a flyover would be as great as 6 PNdB.

Effect of Flap Gap Baffle

The nozzle-flap gap was covered on the lower side by a sheet metal baffle, described above. Figure 31 shows that the acoustical change was small for observation stations directly below the aircraft ($\beta = 0°$). Virtually no effect on noise was produced at the high power setting, and at most, 1.5 PNdB at the nominal approach setting. Spectral comparisons in figure 32 show that the baffle improved the flap shielding capability by several decibels at very high frequencies in the approach

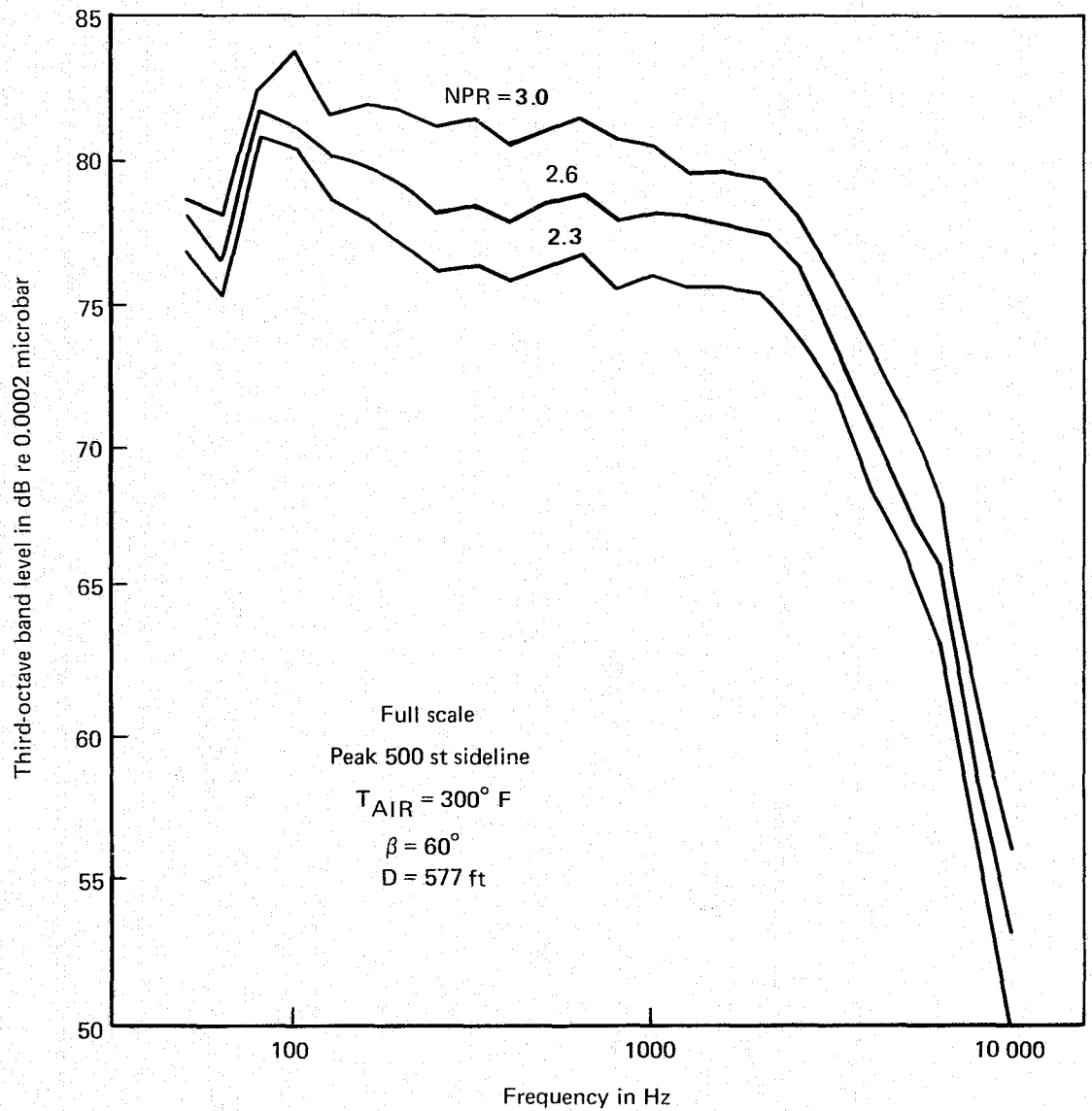

FIGURE 26.—NOISE OF JET FLAP SYSTEM, $\delta_F = 20°$

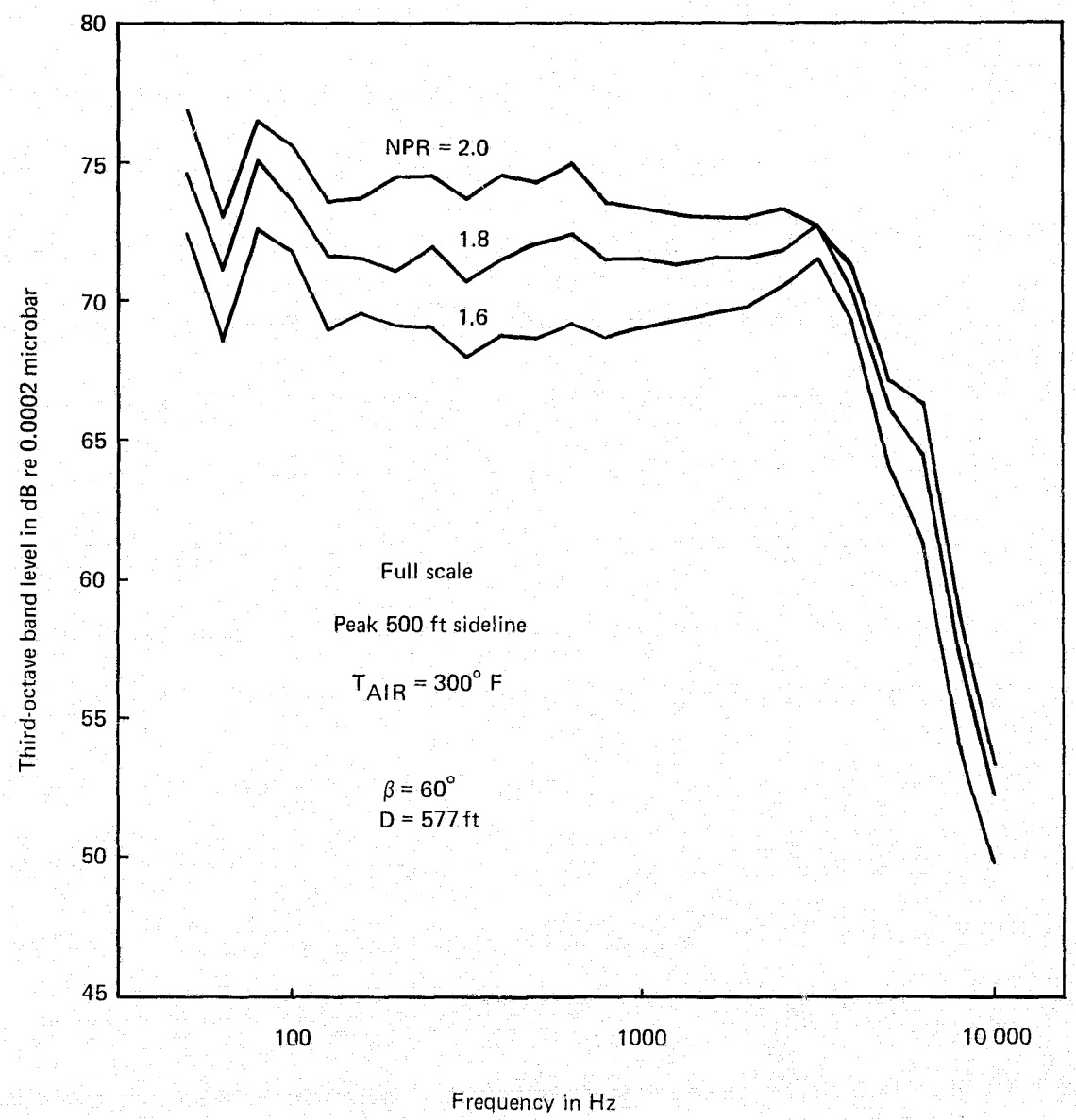

FIGURE 27.–NOISE OF JET FLAP SYSTEM, $\delta_F = 65°$

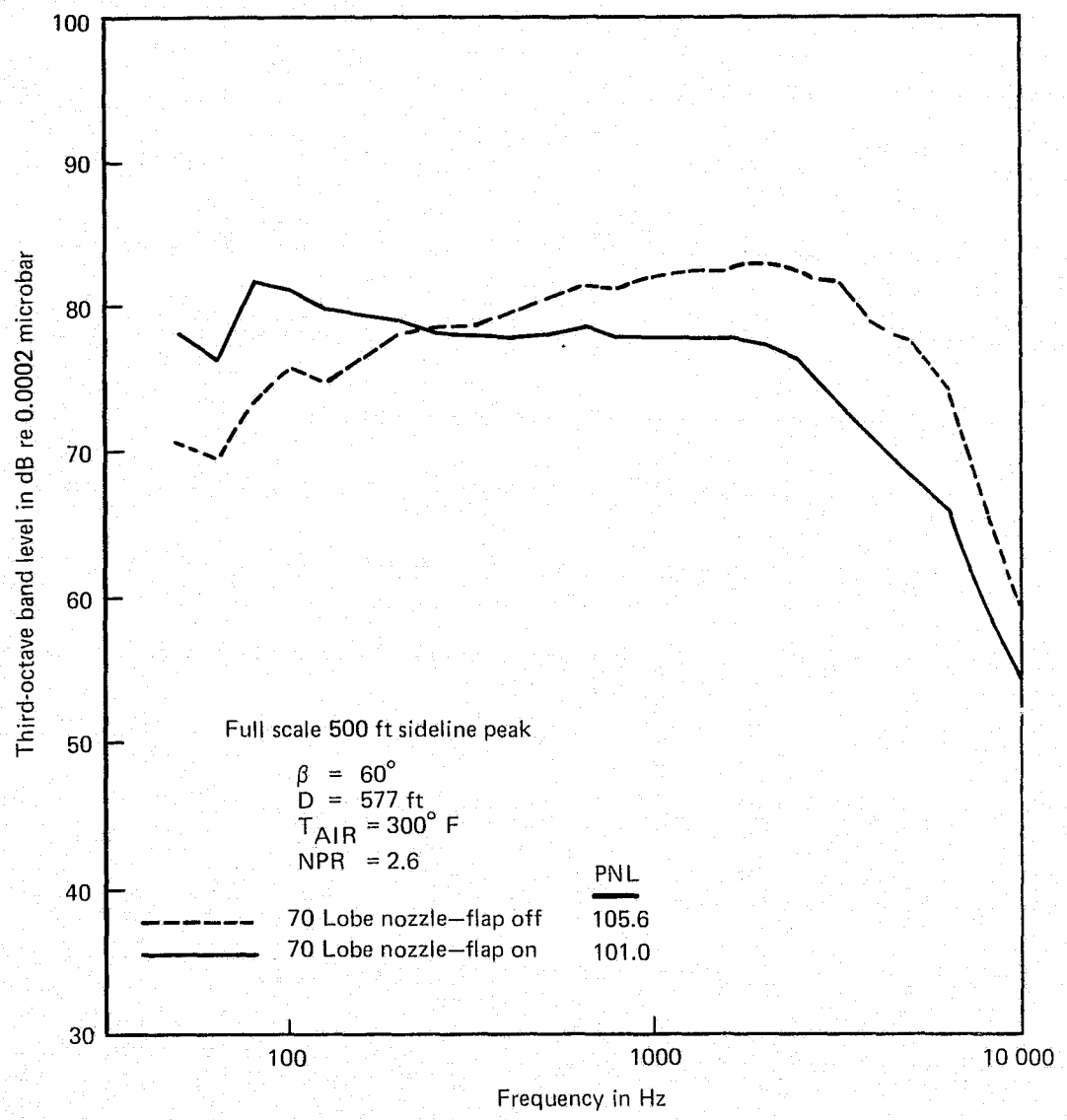

FIGURE 28.—EFFECT OF ADDING JET FLAP (TAKEOFF, $\delta_F = 20°$)

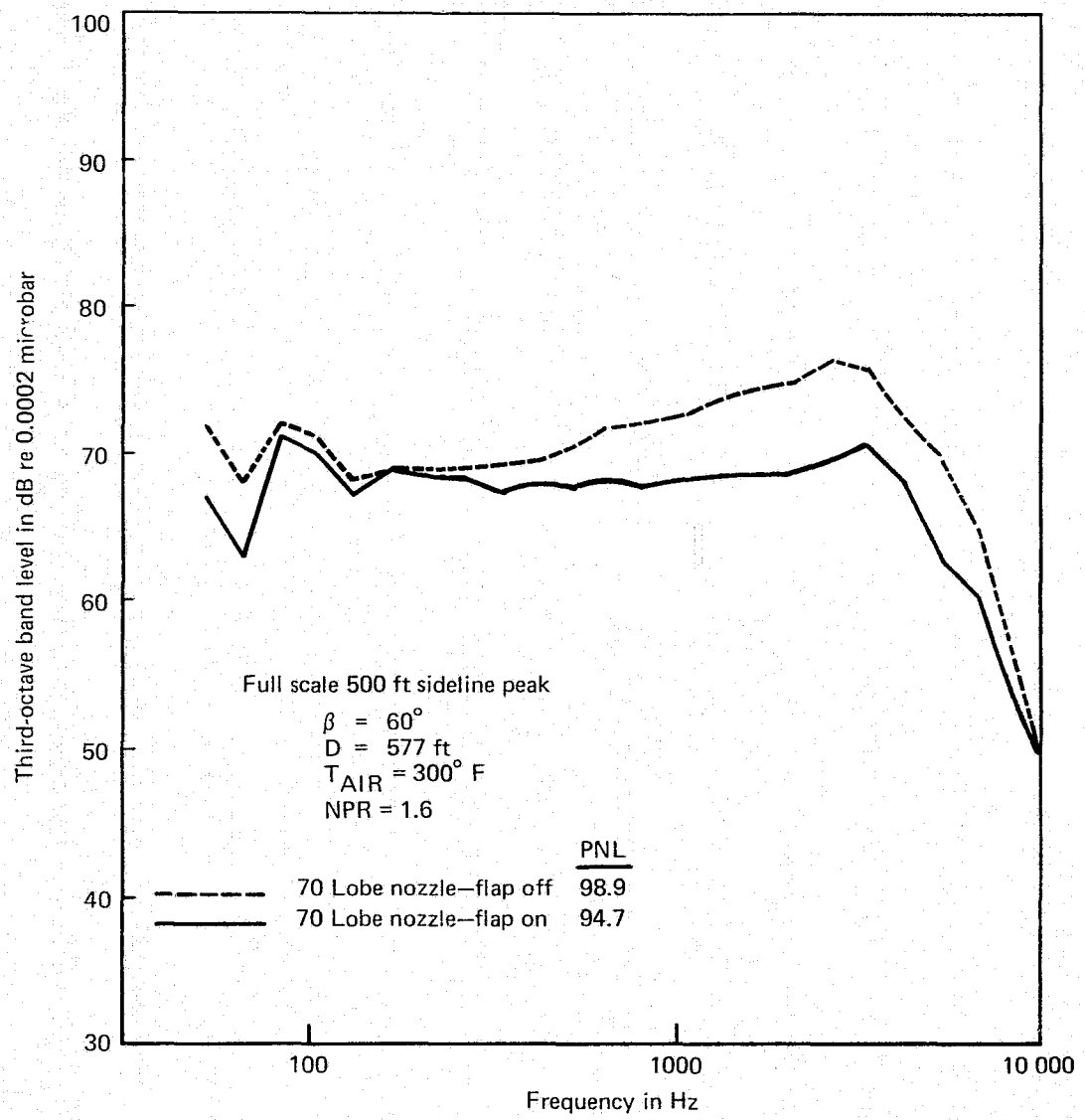

FIGURE 29.—EFFECT OF ADDING JET FLAP (APPROACH, $\delta_F = 65°$)

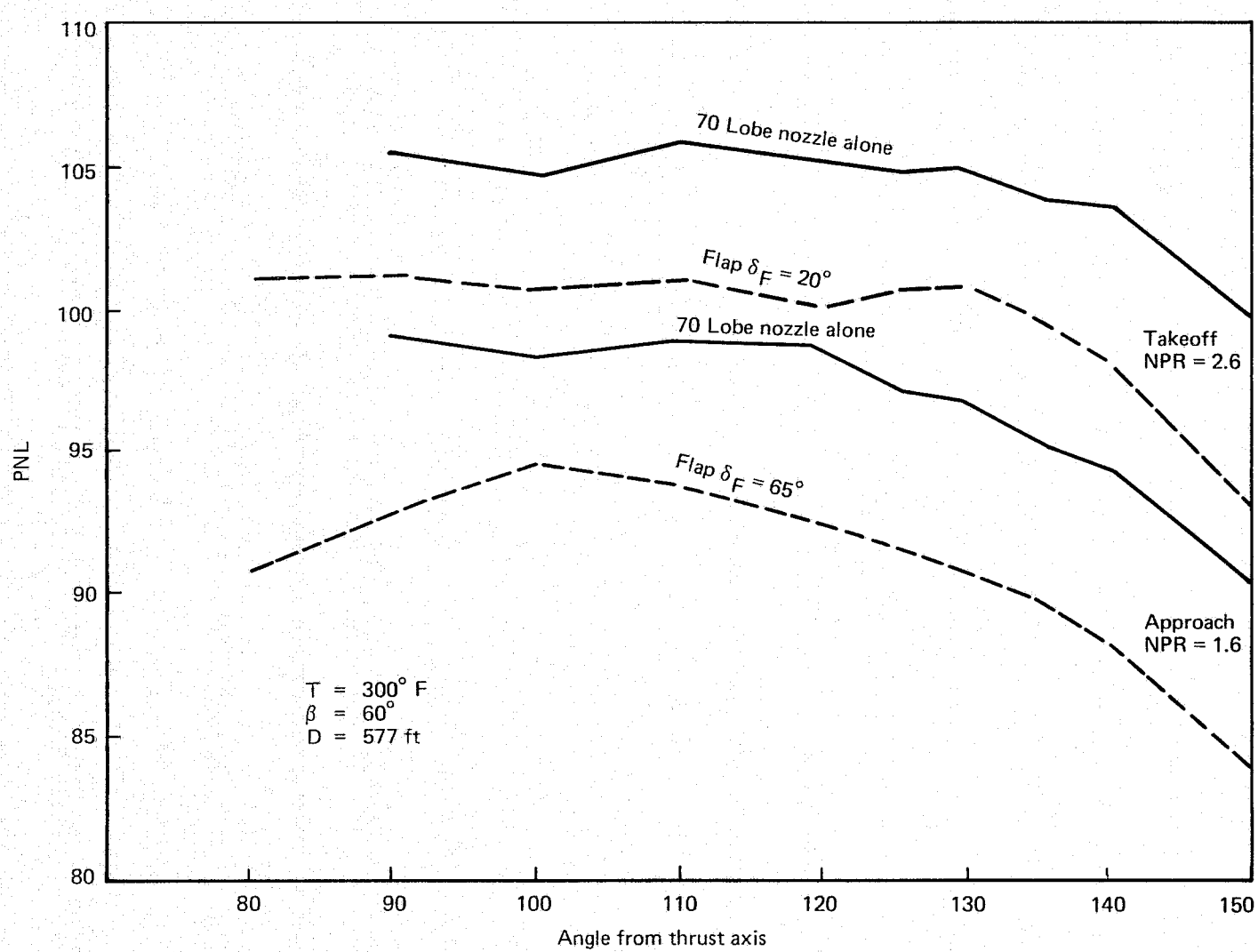

FIGURE 30.—NOISE DIRECTIVITY AT 500 FT SIDELINE

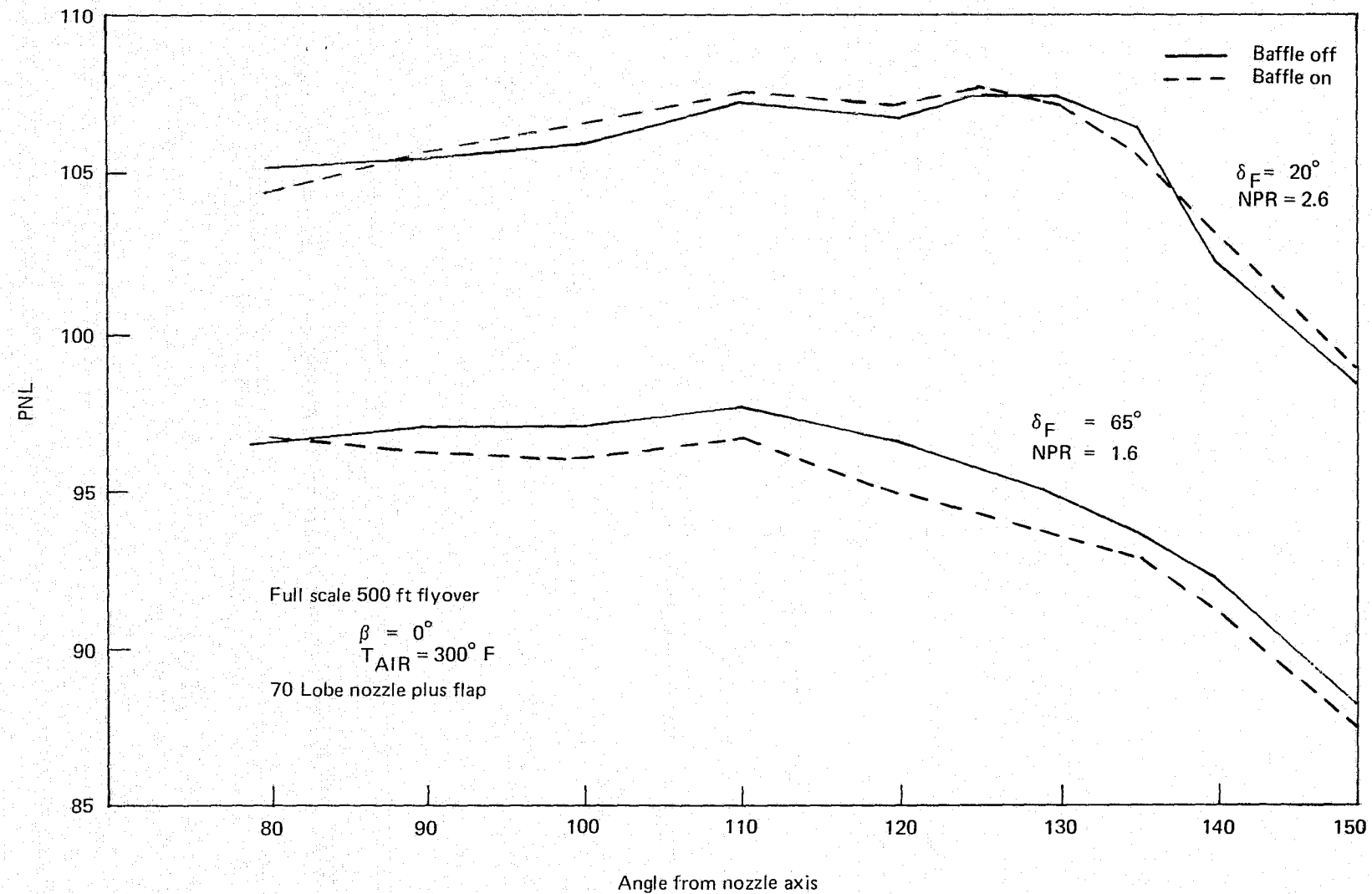

FIGURE 31.—EFFECT OF BAFFLE AT TAKEOFF AND APPROACH FLAP SETTINGS

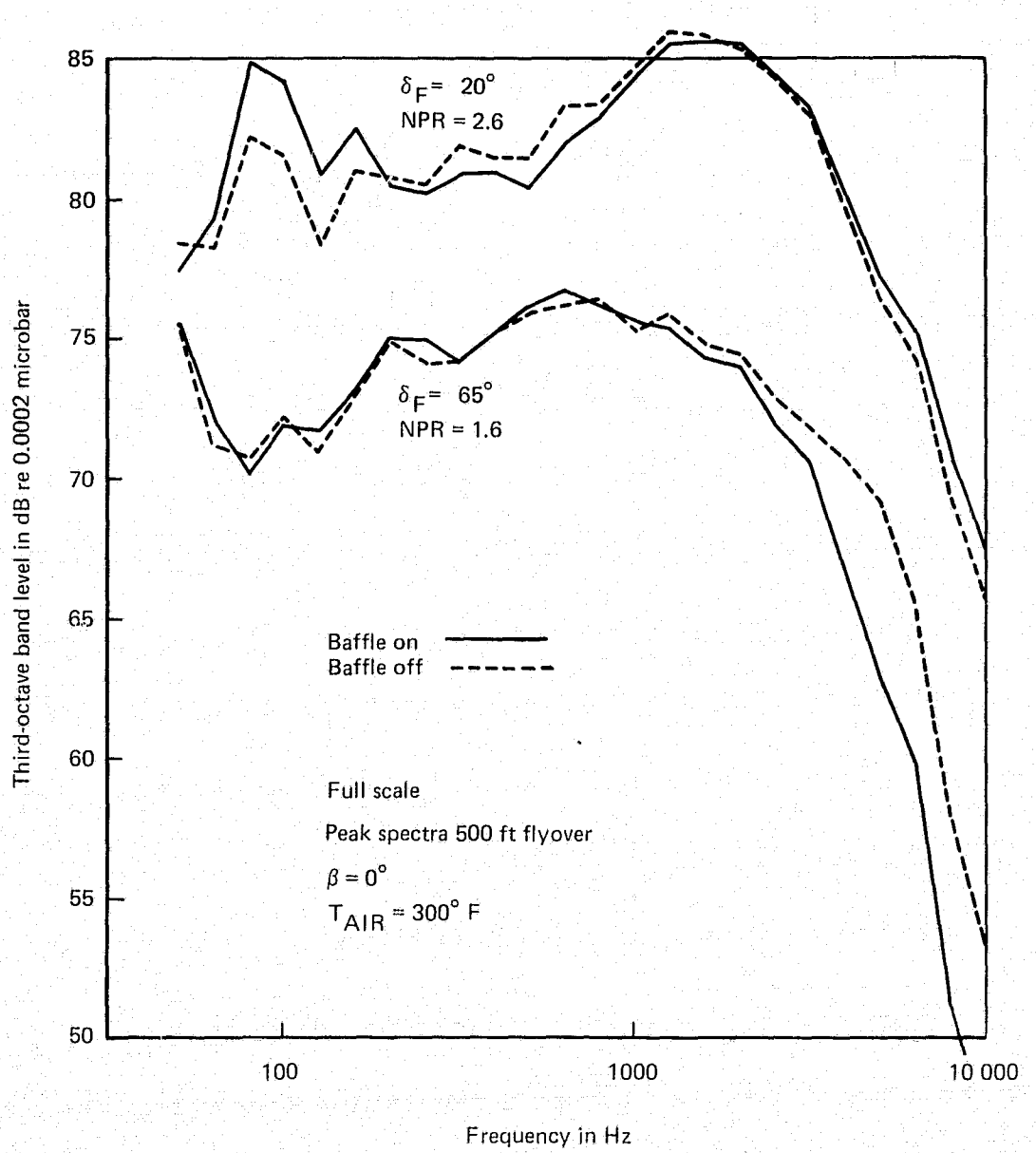

FIGURE 32.—EFFECT OF GAP BAFFLE ON PEAK NOISE SPECTRA

case and hardly at all in the takeoff case. The conclusion is that the nozzle-to-flap opening was not an important sound transmission path.

Comparison With Augmentor Flap

The jet flap with multi-element lobed nozzle array produced promising noise results compared to the augmentor wing flap models tested in the Augmentor Wing Design Integration and Noise Studies (DNS) Tasks V and VIIC (ref. 1 and 3).

Figure 33 compares peak full-scale airplane noise spectra of the jet flap of this study with lined and hard-surfaced augmentor flap systems of Task V (ref. 1). The jet flap, with no special treatment to make it quiet beyond the choice of nozzle array configuration, has demonstrated noise levels which are some 4 PNdB higher than those of the lined augmentor. This augmentor system is the one shown to be capable of meeting a noise goal of 90 PNdB at the 500-ft sideline. It is not unreasonable to think that the application of nozzle corrugations, such as were used on the 20-lobe nozzle of the augmentor system, or some other noise reduction devices or treatments on the jet flap, could make it competitive with the augmentor flap.

The comparison at the landing approach condition is more favorable to the jet flap; its noise is within 0.5 PNdB of the corresponding lined augmentor measurement of DNS Task VIIC (ref. 3). This peak noise comparison is shown in figure 34.

In both figures 33 and 34, the application of acoustic lining to the flow passages in the augmentor flap system is seen to produce some 5 or 6 dB reduction in peak (high-frequency) noise levels. The unlined augmentor system demonstrates greater high-frequency noise than the jet flap does, indicating that the augmentor flap and shroud serve to channel this nozzle-produced noise down through the augmentor exhaust exit instead of reflecting it upward and away. The jet flap leaves the jet flow unshrouded above and partially shields the ground observer from nozzle-generated high-frequency noise.

The jet flap has an apparent disadvantage in low-frequency noise, particularly at the takeoff jet velocity (approximately 1475 ft/sec) condition. The closed-channel augmentor system apparently does not allow jet turbulence interaction noise generation mechanisms of the strength experienced with the single-surfaced jet flap interaction. At the approach condition (V_{jet} approximately 1070 ft/sec), the jet flap interaction noise at low frequency is not as evident or as important. In fact, figure 34 indicates that the low-frequency noise from the augmentor flap system is actually greater at this jet velocity. Perhaps the augmentor acts as a propagation channel for noise produced at or near the nozzle at these low frequencies. It is also possible that the augmentor lower flap produced more interaction noise at the 65° setting simply because it had a sharper leading edge and

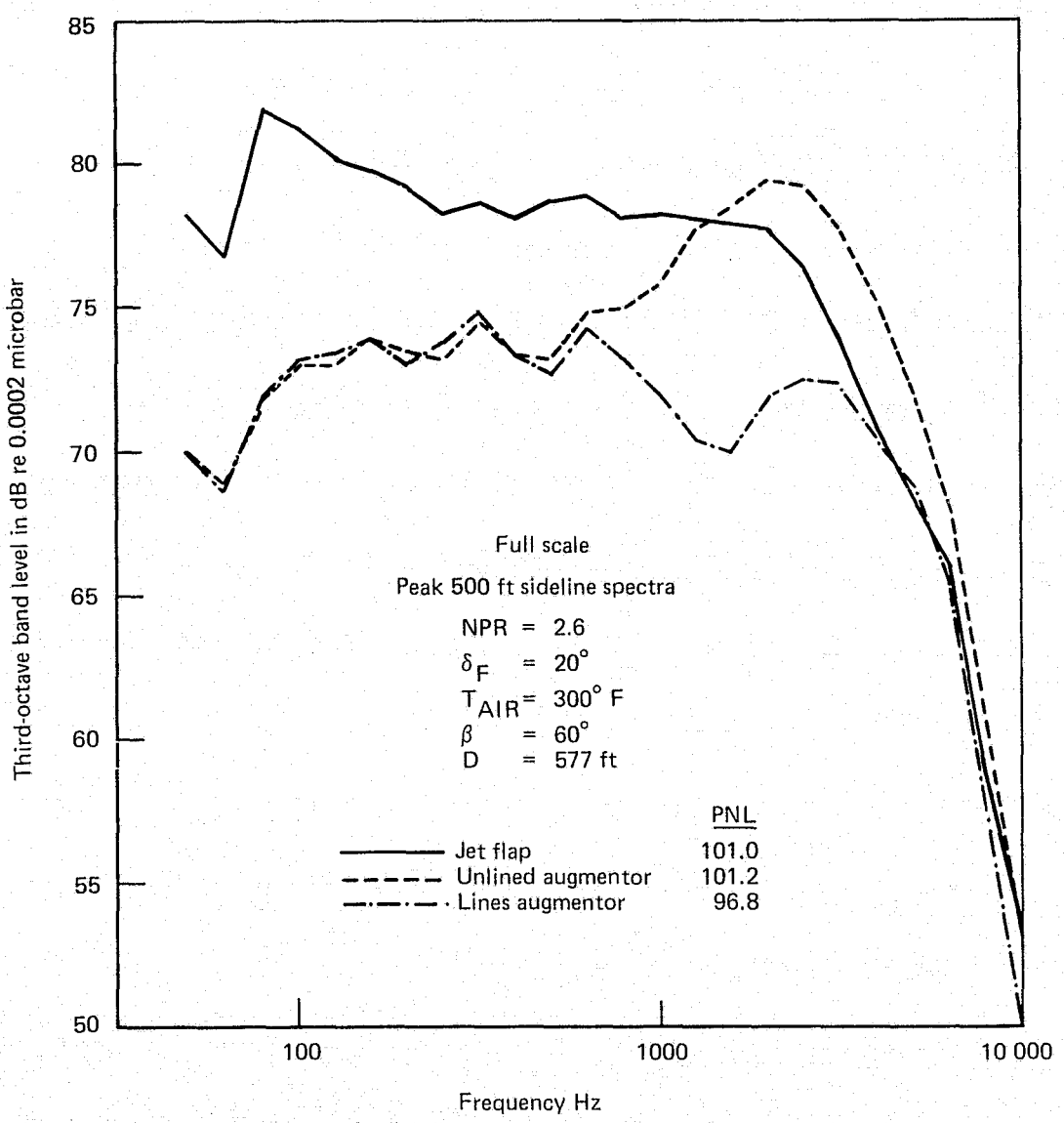

FIGURE 33.—COMPARISON OF JET FLAP TO AUGMENTOR SYSTEM, TAKEOFF CONFIGURATION

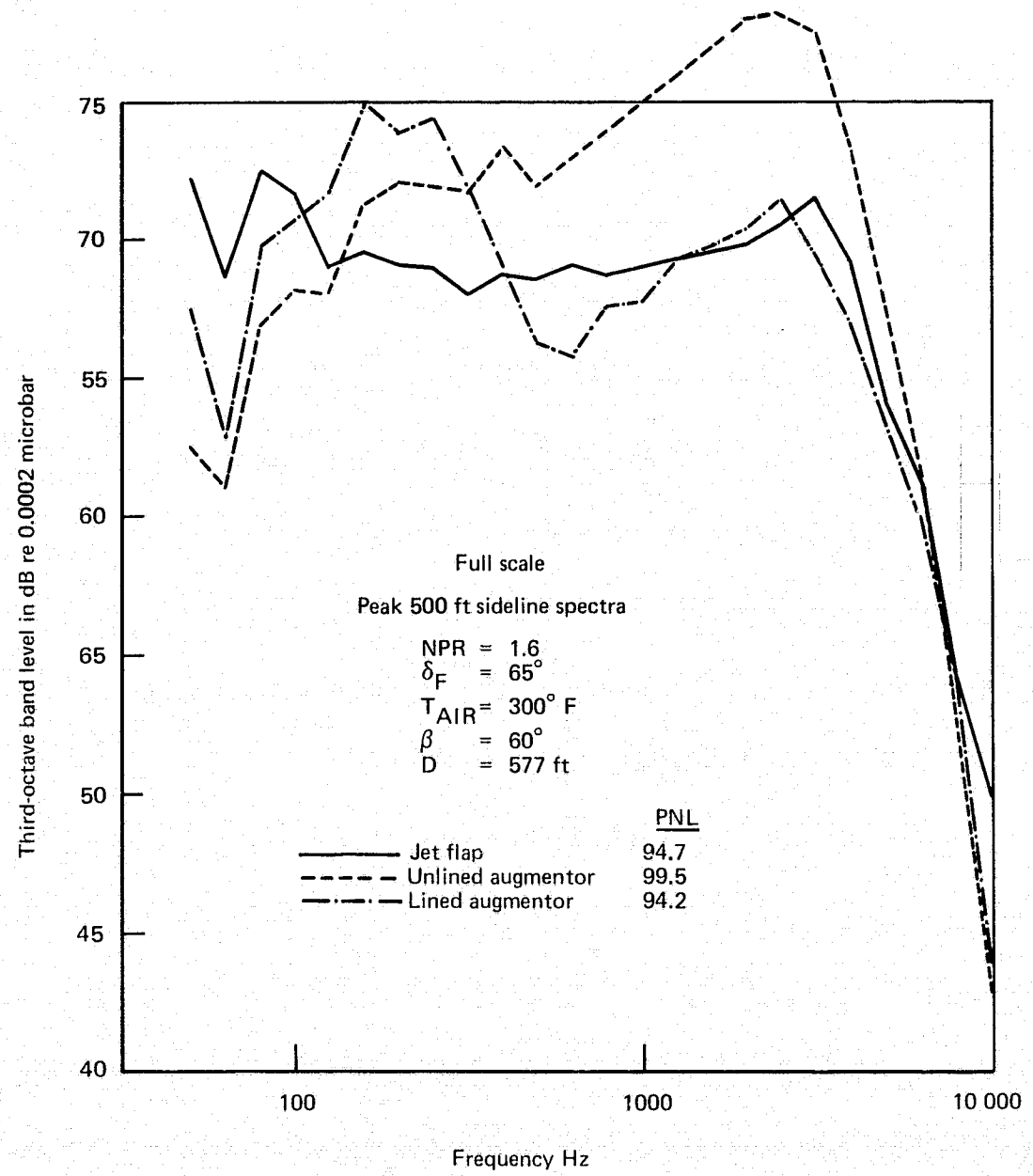

FIGURE 34.—COMPARISON OF JET FLAP TO AUGMENTOR SYSTEM, APPROACH CONFIGURATION

required more projection into the jet flow than did the jet flap. Radius of curvature of the augmentor flap leading edge was dictated by wing stowage considerations, and some direct impingement of the jet onto the flap was found necessary to maintain flow attachment at the high deflection angles. The increased low-frequency noise of the lined augmentor over the hardwall version (fig. 34) might be attributed to the surface roughness introduced by acoustic lining material, although this same noise difference was not seen in the takeoff condition (fig. 33).

In summary, the jet flap is seen to be competitive with the best demonstrated augmentor wing configuration on a community noise basis. It appears that the jet flap may actually have certain noise advantages at low jet velocity, high flap deflection conditions.

Static Performance

Nozzle Alone

The nozzle alone static performance is presented in figure 35. As indicated in the upper figure, the peak velocity coefficient (C_V) is 0.95 for ambient and 300° F air flow temperatures. This is somewhat lower than the performance expected for a nozzle of this design without the splitter screech shields. The splitter screech shields, which bisect each lobe exit, apparently result in about a 2% thrust loss.

The nozzle discharge coefficient level is shown in the lower figure. The peak C_D level measured is about 0.98, which includes the uncertainty of the measured exit area.

Nozzle Plus Flap

Effect of Z position on Static Performance ($\delta_F = 20°$).—The effect of the longitudinal position (ℓ_Z) of the flap relative to the nozzle was not tested here but was selected as optimum from previous tests conducted on similar configurations (ref. 1, 2, and 3). Also demonstrated in the above reference tests is the sensitivity or flow attachment to the perpendicular distance from the coanda surface to the nozzle jet flow (Z position). The effect of Z position on system thrust recovery for the jet flap at takeoff is shown in figure 36. As the Z position is increased, the resultant thrust increases to a value of 2% greater than the nozzle thrust. Some thrust augmentation is realized because of the induced flow along the flap coanda surface which provides a positive pressure/area term across the flap. This more than makes up for the viscous losses which are reduced at the larger Z positions.

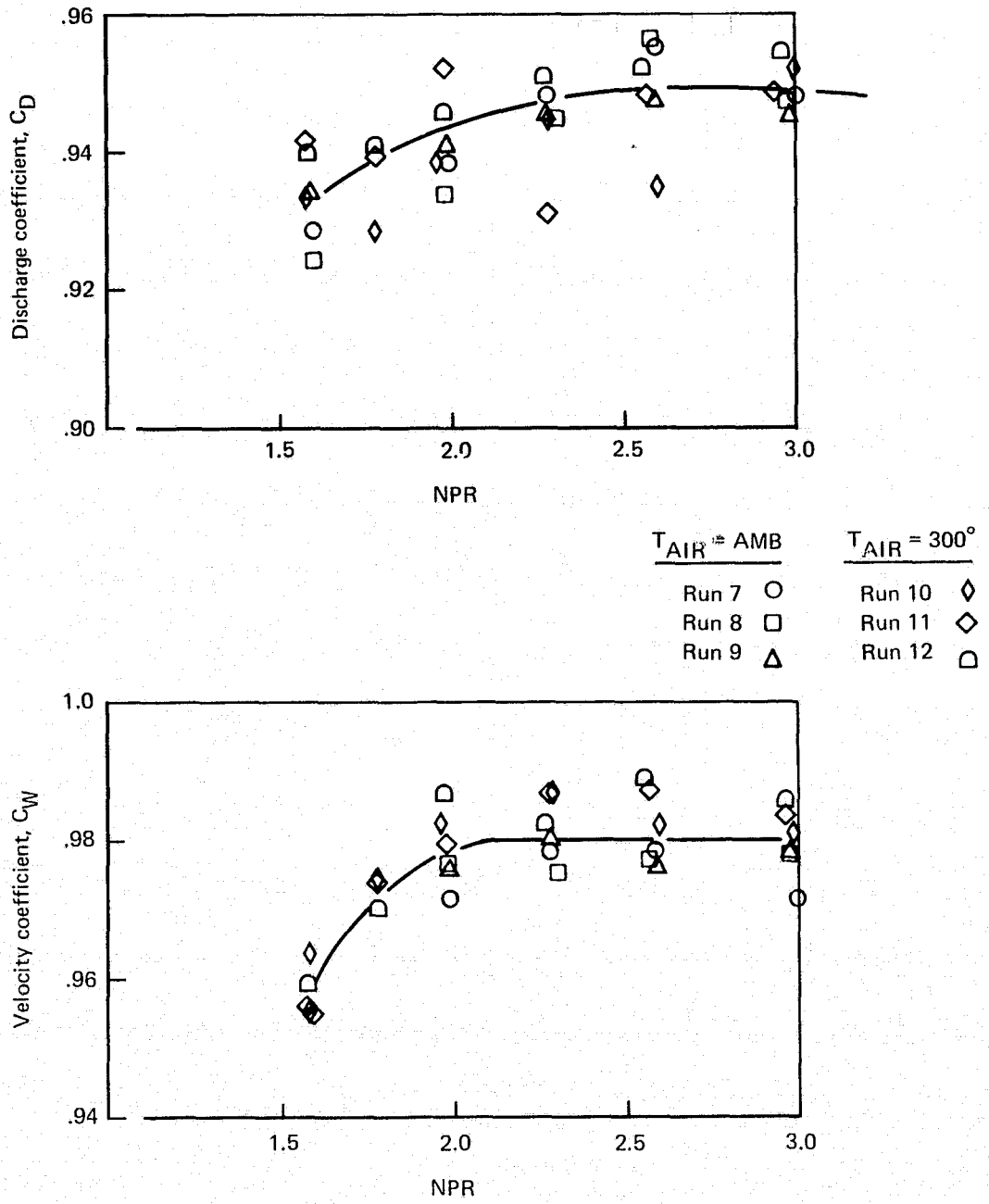

FIGURE 35.–STATIC PERFORMANCE OF 70 LOBE NOZZLE

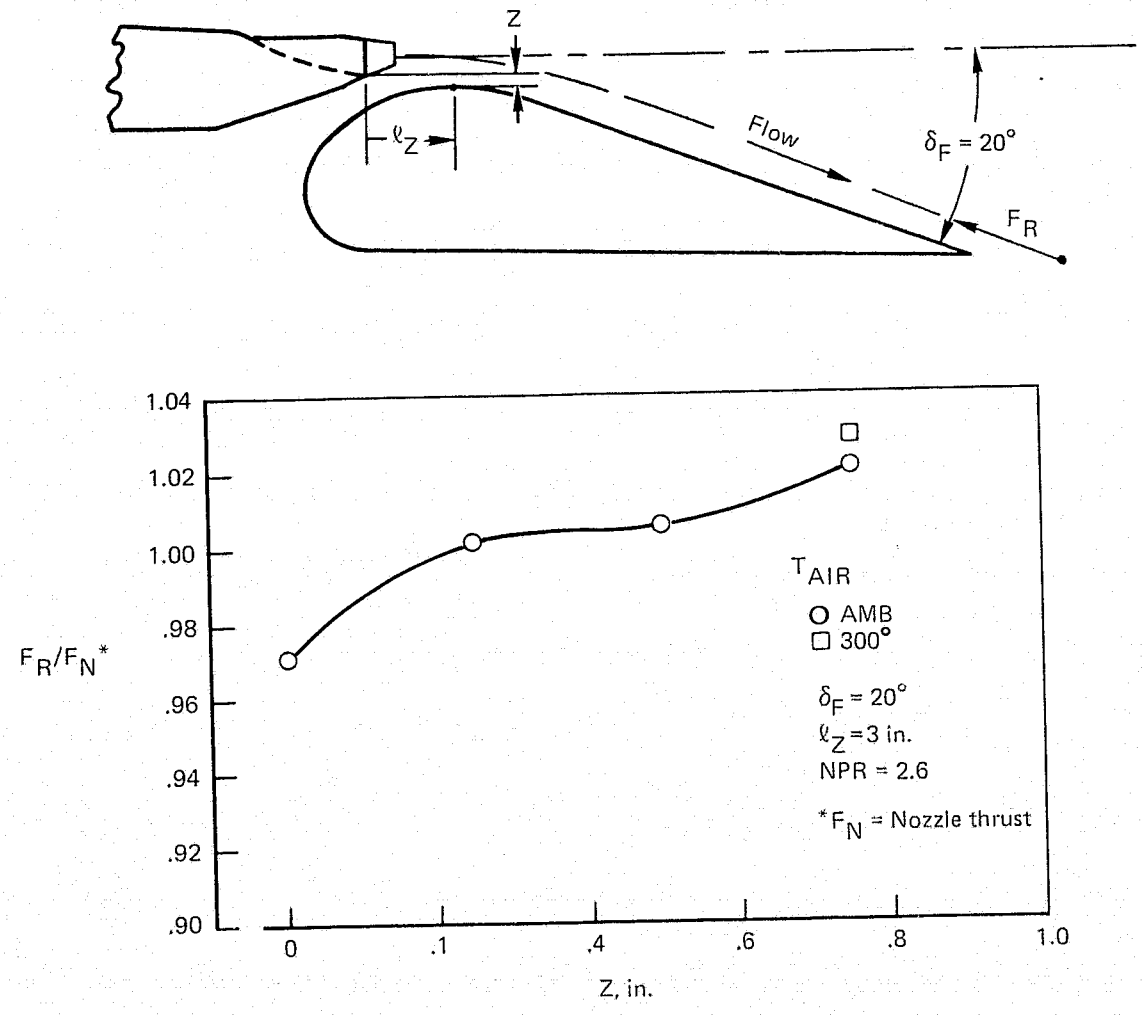

FIGURE 36.—EFFECT OF NOZZLE/FLAP Z POSITIONS ON STATIC PERFORMANCE, $\delta_F = 20°$

Effect of Flap Gap Baffle on Performance ($\delta_F = 20°$ and 65°).—As discussed earlier, flyover noise measurements ($\beta = 0$) were made with and without the baffle covering the gap between the nozzle and the flap. Tests were conducted at both takeoff and approach flap settings. The effects of the baffle on static performance are shown in figure 37. At the takeoff flap setting, a 7% loss in resultant thrust is measured with the baffle installed. The partial ejector action that is experienced with the gap open is eliminated when the gap is sealed, preventing the occurrence of any induced flow. At the approach flap setting, the thrust loss is only about 2% because the amount of induced flow is very small in the "gap open" case.

Jet Turning Effectiveness ($\delta_F = 20°$ and 65°).—The jet turning effectiveness at the takeoff and approach flap settings are shown in figures 38 and 39, respectively. At the takeoff flap setting, jet flow attachment is not particularly sensitive to the Z position, and the turning angle is within 2° of the flap angle for all Z positions tested. With the nozzle air heated to 300° F for the acoustic tests, the turning angle was measured the same as the flap angle (20°).

As indicated in figure 39, flow turning effectiveness or flow attachment is quite sensitive to Z position at the approach flap setting of 65°. If the flap coanda surface is not impinged by the jet (Z position too large), separation of the flow occurs. Flow attachment is attained by positioning the flap closer to the jet, resulting in flow impingement.

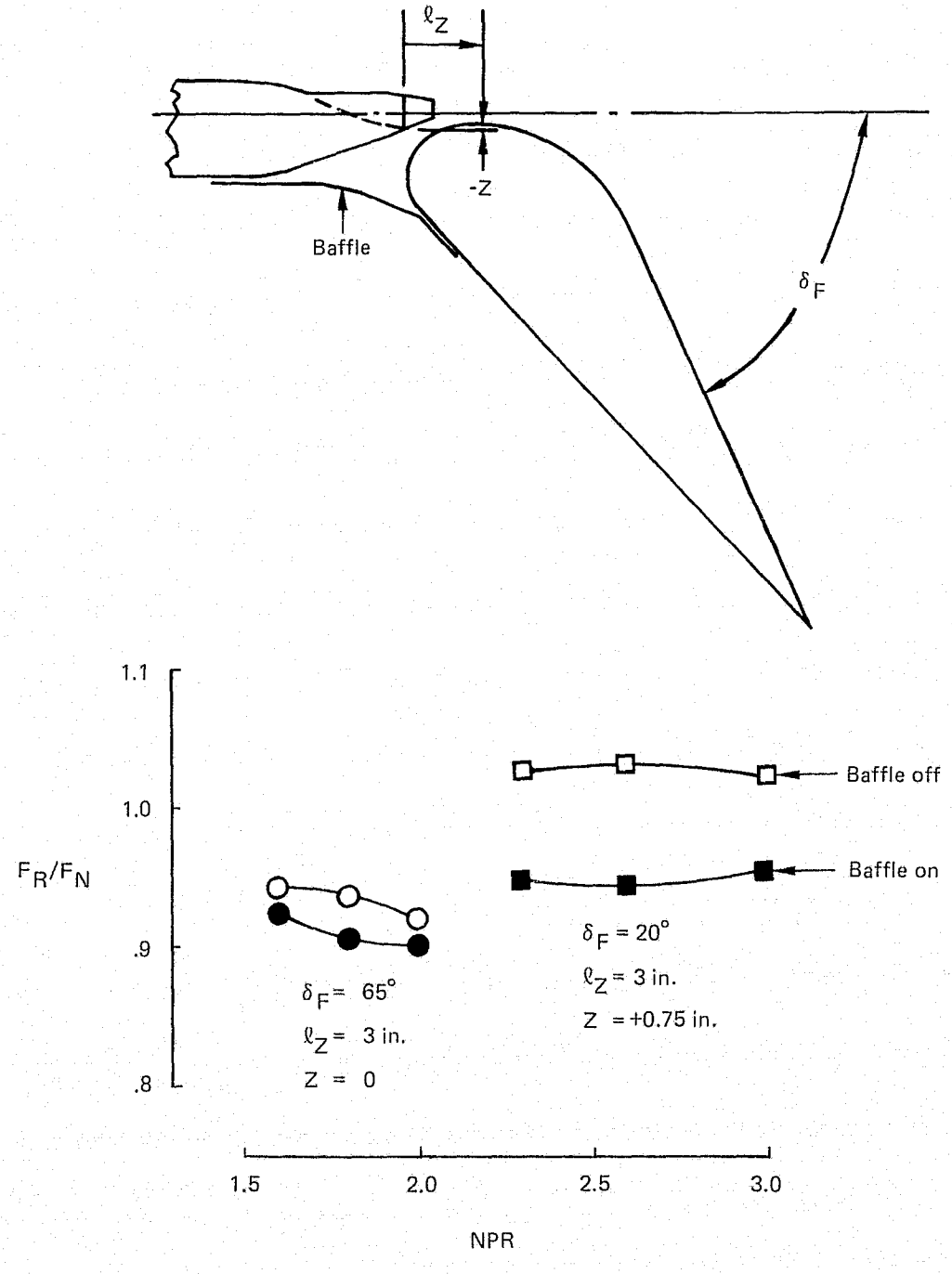

FIGURE 37.—EFFECT OF COVERING NOZZLE/FLAP GAP, δ_F = 20° AND 65°

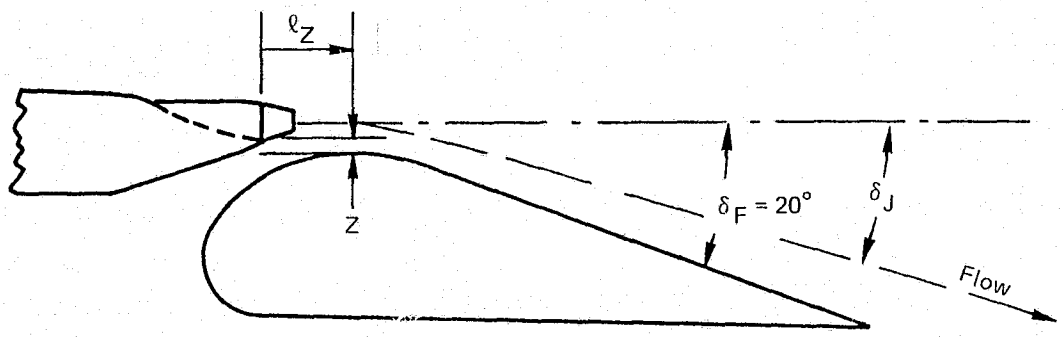

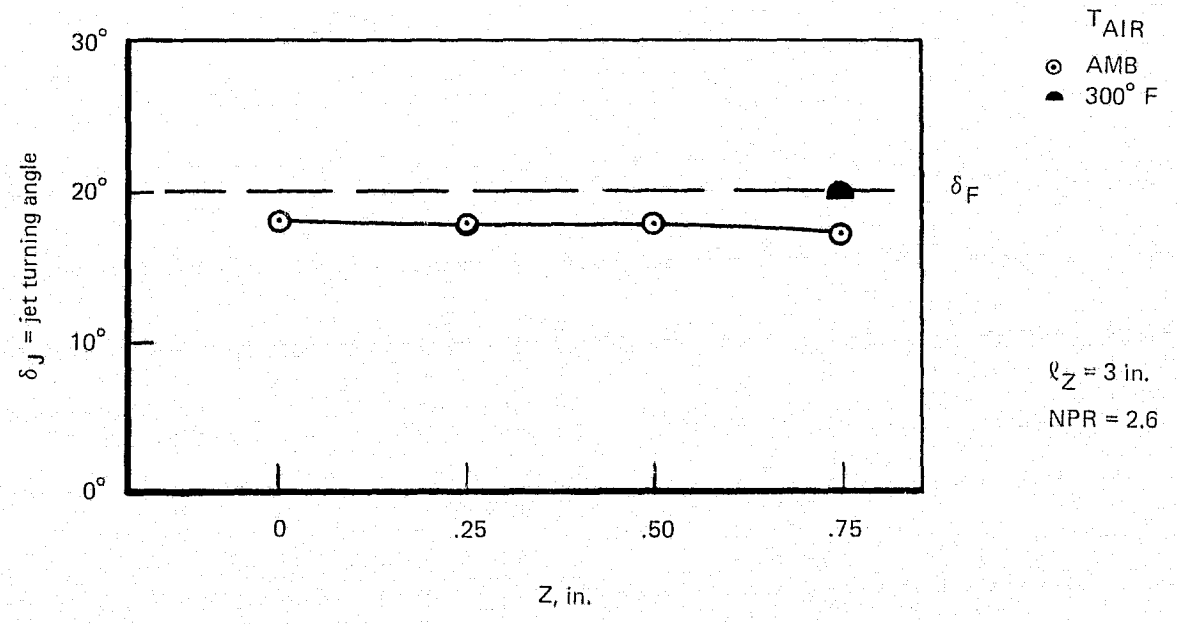

FIGURE 38.–EFFECT OF NOZZLE/FLAP Z POSITION ON JET TURNING ANGLE, $\delta_F = 20°$

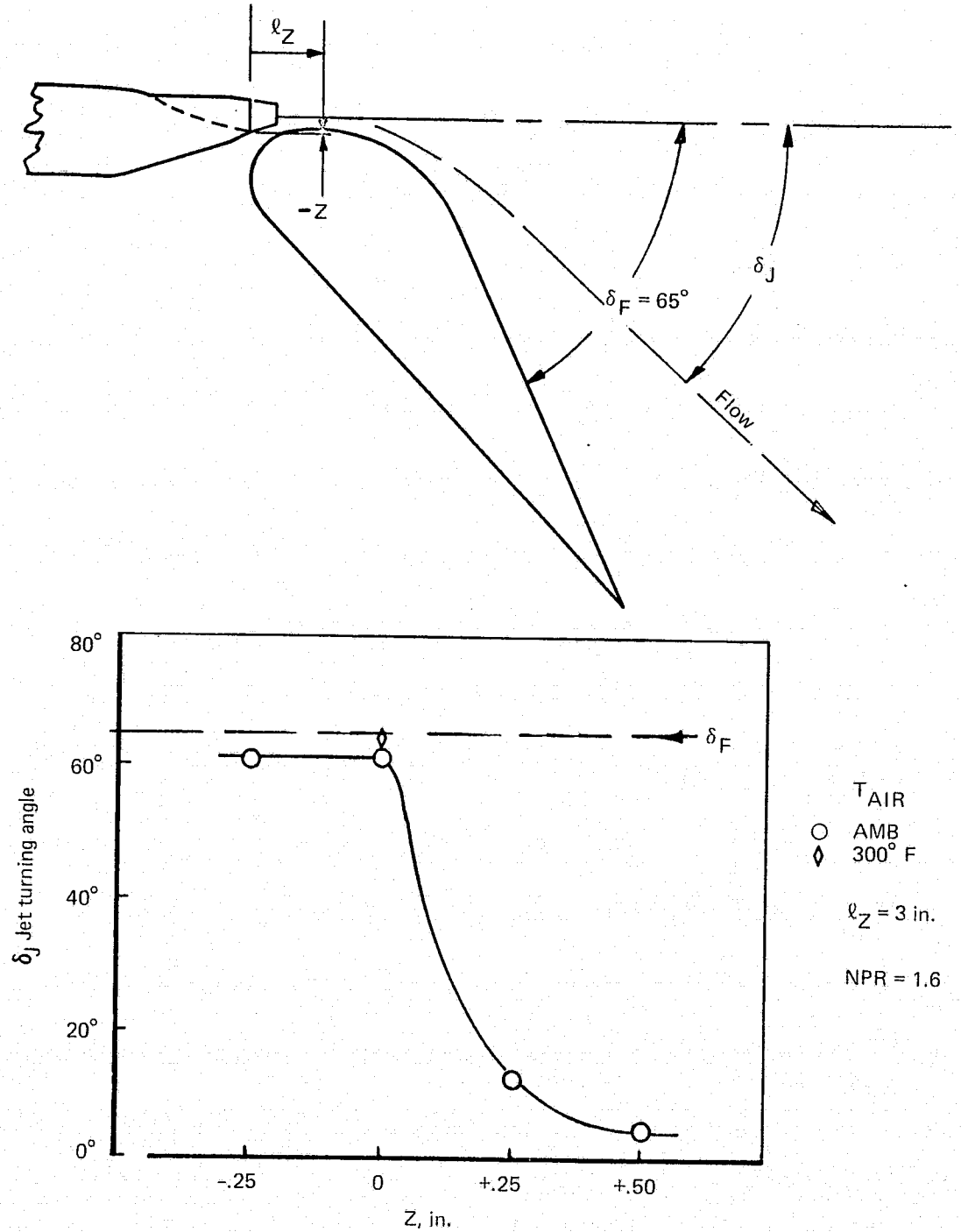

FIGURE 39.—EFFECT OF NOZZLE/FLAP Z POSITION ON JET TURNING ANGLE, $\delta_F = 65°$

CONCLUSIONS AND RECOMMENDATIONS

Analysis of results from static test of the 1/4-scale model jet flap and a multi-element lobe nozzle has shown:

1. The addition of a blown flap to a jet nozzle results in shielding of high-frequency noise sources from observers below the airplane, but low-frequency noise sources are created apparently by jet exhaust turbulence interaction with the flap.

2. A 150-passenger airplane with the jet flap system produces a 500-ft sideline takeoff noise level of 101 PNdB for the configuration tested. This is about 4 PNdB noisier than an equivalent lined augmentor flap system tested previously. The jet flap system is estimated to have a noise potential of 95 PNdB with further research and development, and the augmentor flap airplane was shown to have the potential of achieving 90 PNdB peak noise at the 500-ft sideline on takeoff.

3. The jet flap blown by a multi-element lobe (AAR = 2.7) suppressor nozzle with splitters (screech shields) is as quiet in the landing approach configuration as the corresponding lined augmentor flap model previously tested in the Augmentor Wing DNS Program.

4. Further investigations of a distributed blowing system for STOL aircraft should include consideration of a jet flap system as the noise levels are comparable to a lined augmentor while offering a significant reduction in complexity.

REFERENCES

1. Campbell, J. M.; Harkonen, D. L.; Lawrence, R. L.; O'Keefe, J. V.: *Task V—Noise Suppression of Improved Augmentors for Jet STOL Aircraft,* Final Report, D6-60174, The Boeing Company. NASA CR-114534, January 1973.

2. Campbell, J. M.; Lawrence, R. L.; O'Keefe, J. V.: *Design Integration and Noise Studies for Jet STOL Aircraft* Final Report, Volume III—Static Test Program, D6-40552-3, The Boeing Company. NASA CR-114285, May 1972.

3. Campbell, J. M.; Harkonen, D. L.; O'Keefe, J. V.: *Task VIIC Augmentor Wing Cruise Blowing Valveless System* Volume I. Static Test Program, D6-41216, The Boeing Company. NASA CR-114623, November 1973.

4. Roepcke, F. A.; Nickson, T. B.: *Task VIIA, Augmentor Wing Cruise Blowing Valveless System,* Volume I., System Design and Test Integration, D6-40950, The Boeing Company. NASA CR-114621, April 1973.

5. *Design Integration and Noise Study for a Large STOL Augmentor Wing Transport*—Task I Report, D6-60139, The Boeing Company. NASA CR 2-634, July 1971.

6. Dorsch, R. G.; Reshoto, M.; Olsen, W. A.: *Flap Noise Measurements for STOL Configurations Using External Upper Surface Blowing,* AIAA Paper 72-1203, 1972.

7. Maus, J. R.; Schrecker, G. O. *Noise Characteristics of Jet Flap Type Exhaust Flows.* NASA CR-2342, February 1974.